AGU ADVANCING EARTH AND SPACE SCIENCE

Water Resources Research

RESEARCH ARTICLE
10.1029/2022WR033305

Hydroclimate Drives Seasonal Riverine Export Across a Gradient of Glacierized High-Latitude Coastal Catchments

J. Jenckes[1,2], L. A. Munk[1], D. E. Ibarra[3,4], D. F. Boutt[5], J. Fellman[6], and E. Hood[6]

[1]Department of Geological Sciences, University of Alaska Anchorage, Anchorage, AK, USA, [2]Department of Geosciences, University of Alaska Fairbanks, Fairbanks, AK, USA, [3]Department of Earth, Environmental and Planetary Sciences, Brown University, Providence, RI, USA, [4]Institute at Brown for Environment and Society, Brown University, Providence, RI, USA, [5]Department of Geosciences, University of Massachusetts Amherst, Amherst, MA, USA, [6]Department of Environmental Sciences, University of Alaska Southeast, Juneau, AK, USA

Key Points:

- Solute and sediment yields are dominated by the presence of glaciers in watersheds; however, hydroclimate dictates seasonal cycles
- Glacial recession and increased rain across the Gulf of Alaska will alter the timing and magnitude of solute and sediment flux to the ocean
- Watershed characteristics such as wetland area, vegetated area, and lithology impart strong controls on solute and sediment yields

Supporting Information:

Supporting Information may be found in the online version of this article.

Correspondence to:

J. Jenckes,
jjenckes2@alaska.edu

Citation:

Jenckes, J., Munk, L. A., Ibarra, D. E., Boutt, D. F., Fellman, J., & Hood, E. (2023). Hydroclimate drives seasonal riverine export across a gradient of glacierized high-latitude coastal catchments. *Water Resources Research*, *59*, e2022WR033305. https://doi.org/10.1029/2022WR033305

Received 6 AUG 2022
Accepted 31 MAR 2023

Abstract Glacierized coastal catchments of the Gulf of Alaska (GoA) are undergoing rapid hydrologic fluctuations in response to climate change. These catchments deliver dissolved and suspended inorganic and organic matter to nearshore marine environments, however, these glacierized coastal catchments are relatively understudied and little is known about total solute and particulate fluxes to the ocean. We present hydrologic, physical, and geochemical data collected during April–October 2019–2021 from 10 streams along gradients of glacial fed to non-glacial (i.e., precipitation) fed, in one Southcentral and one Southeast Alaska region. Hydrologic data reveal that glaciers drive the seasonal runoff patterns. The $\delta^{18}O$ signature and specific conductance show distinctive seasonal variations in stream water sources between the study regions apparently due to the large amounts of rain in Southeast Alaska. Total dissolved solids concentrations and yields were elevated in the Southcentral region, due to lithologic influence on dissolved loads, however, the hydroclimate is the primary driver of the timing of dissolved and suspended yields. We show the yields of dissolved organic carbon is higher and that the $\delta^{13}C_{POC}$ is enriched in the Southeast streams illustrating contrasts in organic carbon export across the GoA. Finally, we illustrate how future yields of solutes and sediments to the GoA may change as watersheds evolve from glacial influenced to precipitation dominated. This integrated analysis provides insights into how watershed characteristics beyond glacier coverage control properties of freshwater inputs to the GoA and the importance of expanding study regions to multiple hydroclimate regimes.

1. Introduction

Earth's cold regions are rapidly degrading primarily driven by atmospheric warming. Globally, glaciers are losing mass at an accelerated rate leading to changes in the flux of freshwater, solutes, and sediment (Anderson, 2005; Beamer et al., 2017; Hood et al., 2020; Neal et al., 2010; Zhang et al., 2022). Sediment fluxes have increased in the past several decades in many high latitude, high altitude, and cold regions driven by the deterioration of the cryosphere (Li et al., 2021; Zhang et al., 2022). Glacierized watersheds are extremely important in moderating hydrologic and biogeochemical cycles globally (Milner et al., 2017). Glacier mass loss has increased and accelerated in the 21st century (Hugonnet et al., 2021) and changes to the biogeochemical cycles associated glacier loss is not yet fully understood. High latitude regions, which contain much of Earth's glaciers, are experiencing warming at twice the global rate (IPCC, 2018) driving increases in glacier mass loss.

A high latitude region of particular significance is the Gulf of Alaska (GoA) which supports an extensive biodiversity of marine plants and organisms, subsistence lifestyles of coastal communities and is a globally renown fishery. Glaciers in Alaska are declining at a rapid rate, with a negative mass balance of -75 ± 11 Gt yr^{-1} between 1994 and 2013 (Larsen et al., 2015) leading to an increase of freshwater input to coastal environments. Accordingly, there has been a large amount of recent work to quantify the freshwater and biogeochemical fluxes within high latitude glacierized watersheds (Beamer et al., 2016; Bergstrom et al., 2021; Giesbrecht et al., 2022; Hood & Berner, 2009; Hood et al., 2020; Neal et al., 2010; Sergeant et al., 2020). Physical properties of stream freshwater along with constituent loads of dissolved organic carbon (DOC), particulate organic carbon (POC), and total suspended sediment (TSS) are important parameters to understand how nearshore organisms and ecosystems will change during the coming century (Arimitsu et al., 2016; Whitney et al., 2018). More broadly, freshwater derived from glacier melt is contributing to ocean acidification, due to its low total alkalinity, and enhanced ability to drawdown more CO_2 from the atmosphere (Evans et al., 2014; Reisdorph & Mathis, 2014). The

characterization of riverine material fluxes is an important pathway for investigating how global climate change affects land-to-ocean connections in high-latitude regions.

The GoA receives freshwater, and material fluxes from a large regional coastal drainage basin that spans a perhumid hydroclimate in the southeast to a subpolar hydroclimate in the north. By the end of century, freshwater fluxes derived from glaciers will decrease by 14%–34%, however overall runoff will increase due to increase precipitation in fall and winter rain (Beamer et al., 2017). The coastline of the GoA is characterized by ice covered mountains, rainforest ecosystems, and marine estuaries and fjords influenced by terrestrial water fluxes where the coastal glaciers account for ∼10% of the Earth's mountain glacial cover (Pfeffer et al., 2014). The watersheds of the GoA are undergoing warming air temperatures, increasing rainfall, diminishing snowpack, and rapid glacial recession (Bieniek et al., 2014; Gardner et al., 2013; Shanley et al., 2015), which all contribute to increased freshwater but also to changes in material fluxes from the land to the ocean (Edwards et al., 2021; Sergeant et al., 2020). The freshwater fluxes impact (a) coastal oceanographic patterns (Johnson, 2021), (b) nutrient fluxes critical to the high primary productivity of the coastal waters (Arimitsu et al., 2016; Fellman, Hood, Dryer, & Pyare, 2015), and (c) sediment loads that transfer POC and inorganic sediments to the coastal sedimentary systems (Hood et al., 2020). The sources, transport, and delivery of solute and sediment fluxes are greatly influenced by watershed characteristics (Hood & Berner, 2009; Jenckes et al., 2022; McClelland et al., 2014; Moore et al., 2009). In particular, the presence or absence of headwater glaciers can induce strong seasonal patterns in runoff (Beamer et al., 2017; O'Neel et al., 2015; Sergeant et al., 2020) and glaciers highly influence both chemical and physical weathering (e.g., Alley et al., 2019; Anderson, 2005; Hallet et al., 1996; Koppes & Montgomery, 2009).

Previous watershed-scale studies in the GoA have focused on the biogeochemical properties of stream waters, specifically in Southeast Alaska (Edwards et al., 2021; Fellman et al., 2020, 2014; Hood & Berner, 2009; Hood et al., 2020; Hood & Scott, 2008). However, the land-to-ocean export of geochemical species, such as the major, minor, and trace elements and anionic species that control alkalinity are less well understood but are expected to change as glaciers continue to recede. Mechanical and chemical weathering from glaciers has a profound impact on the flux of major and minor elements transported to the ocean (Urra et al., 2019). For example, dissolved Fe fluxes are lower in glacierized tributaries feed the Copper River (Schroth et al., 2011). Most recently Bergstrom et al. (2021) in study of Wolverine Glacier, in Southcentral Alaska, showed how seasonal Ca^{2+} flux was elevated in the fall due to increased rain compared to a year with limited rain events. Additionally, glacial coverage and geomorphology controls on solute fluxes were explored by Jenckes et al. (2022) within watersheds of the GoA, illustrating that watershed geomorphology (e.g., slope, elevation, relief) drives solute production (concentration-discharge relationships) while glacier coverage controls the overall yields of solutes.

Sediment transported to the GoA likely provides micronutrient fluxes to nearshore ecosystems (Bhatia et al., 2013; Hawkings et al., 2018; Raiswell et al., 2006). Changes in the future sediment yield are not well constrained within the GoA, however, sediment yields from glacial influenced streams can be elevated, especially within the GoA region (Hallet et al., 1996). Associated with these large yields of glacier derived sediment are potential sources of micronutrient (i.e., Fe) bearing particles (Hawkings et al., 2018). Though detailed work is limited within GoA rivers, based on previous studies in other Arctic regions glacierized catchments maybe a significant source of micronutrients for primary productivity provided by the large sediment fluxes (Bhatia et al., 2013; Hawkings et al., 2018; Raiswell et al., 2006). Therefore, it is important to investigate the variability of sediment load across the GoA to better conceptualize future changes to nearshore ecosystems.

Currently, within Southeast Alaska stream discharge has yet to reach peak water from glacier melt (Young et al., 2021). As watersheds lose glacial ice they evolve and develop vegetative cover and soils and increase storage of organic carbon (Buma & Barrett, 2015; Chandler, 1943). Although much work has been done on the details of freshwater flux and organic carbon dynamics in southeast GoA coastal catchments (e.g., Edwards et al., 2021; Hood et al., 2020), there is limited information on the contributions to the subpolar region of the GoA (i.e., Southcentral Alaska) which is also undergoing transformation due to climate change. Therefore, the focus of our study is a detailed investigation of how the seasonal patterns and yields of solutes and sediments (organic and inorganic fractions) compare across (a) a gradient of glacier coverages and (b) hydroclimate regimes. As the hydroclimate in the GoA shifts, the subpolar region of the GoA will experience increased precipitation as rain in the fall likely evolving to a similar precipitation regime as the Southeast. We use data collected within two regions (a) Kachemak Bay (KB) situated in the northern GoA and (b) Lynn Canal (LC) in southeast Alaska (Figure 1).

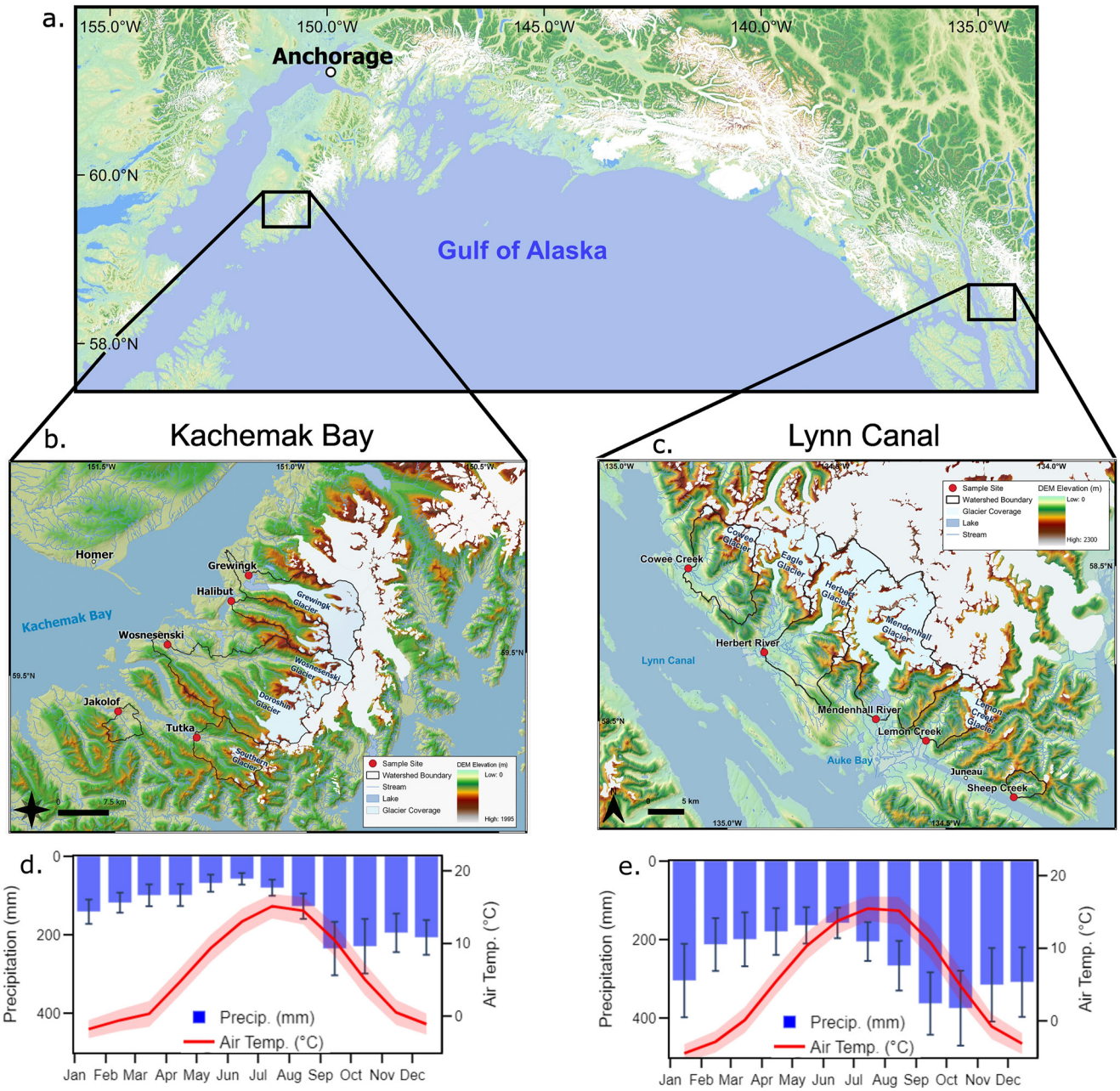

Figure 1. Study areas within the perspective of the Gulf of Alaska (a), Kachemak Bay (b) study watersheds located in Southcentral Alaska and Lynn Canal (c) study watersheds located in Southeast Alaska. Each study area contains a gradient of glacierized to non-glacierized catchments. Across the two study areas there exists a hydroclimate gradient as illustrated in the precipitation records for Kachemak Bay (d) and Lynn Canal (e). Precipitation and air temperature are averages from 1991 to 2020 acquired from DAYMET V4. Variability of precipitation and air temperature are represented by standard deviation with error bars for precipitation and shaded area for air temperature. The Lynn Canal study sites receive approximately twice the precipitation compared to the Kachemak Bay sites, and is on average slightly warmer.

Our approach is to use a unique dataset of stream discharge, solute, and suspended sediment data collected monthly April–October 2019–2021. The data presented here is the first published data from the KB study region and therefore expands on the longer-term studies conducted exclusively in the LC region. We first use seasonal hydrographs, specific conductance, and stable water isotopes, to explore the seasonal differences in water sources to stream freshwater discharge across the glacial gradient of watersheds. Second, within the context of the distinct lithology, landcover, and hydroclimates, we show how the seasonal dynamics of dissolved a suspended material concentrations and yields differ between the two study regions and propose major processes and controls on these

differences. Finally, we conceptualize hypothetical future trends in solute and sediment yields within the GoA region formulated on the observations and analysis presented.

2. Study Region

The KB and LC study areas are located at the western and eastern edges of the GoA, respectively (Figure 1). The two regions have distinct underlying lithologies, different hydroclimate regimes, differ in drainage basin size, percent glacierization, and vegetative cover. KB is situated at the southern end of the Kenai Peninsula in South Central Alaska; at its mouth it is 39 km wide, 63 km in length, and adjoins the southern Cook Inlet. The bathymetry of the bay is relatively flat and averages 46 m deep, however, a trench approximately 160 m deep runs along the southern shore. The south side where the watersheds of interest for this study are located is characterized by steep glacial and postglacial topography of the Kenai Mountains. The LC study watersheds lie in the Coast Mountains and drain directly into the east side of the fjord. At 140 km long and over 600 m deep, LC is the longest and deepest fjord in North America.

2.1. Geology

KB is located along an active subduction zone that dips beneath south-central Alaska and the Aleutian Volcanic Arc (Bradley et al., 1999). Geology of the KB watersheds is characterized by the McHugh Complex, which is a melange within the Chugach Terrane, a Mesozoic-Cenozoic accretionary prism derived from offscraping of the Peninsular-Wrangallia-Alaxander superterrane (Kusky & Bradley, 1999). In the study area, the McHugh Complex is divided into three distinct units (defined in Text S2 in Supporting Information S1). The major lithologies in the McHugh Complex are greywacke, conglomerate, mélange, limestone, chert, argillite, gabbro, and ultramafic rocks which are deformed up to blueschist facies. Additionally, obduction emplaced an ophiolite complex within the region. Intrusions of younger plutons and dikes are present throughout.

The LC study area is located in northern Southeast Alaska. A prominent feature is the Juneau Icefield which covers 3,000 km^2 of the Coast Mountains. Landscape features include glaciers, steep valleys, wetlands, and glacial till covered in forest (D'Amore et al., 2012). Most of the glacial ice sits on intrusive rocks of the coast plutonic-metamorphic complex (Nagorski et al., 2021) which is comprised mainly of intermediate tonalite and diorite, dominated by hornblende, biotite, and quartz. Immediately down gradient of the glaciers, the geology is characterized by metamorphic rocks including chlorite schist, biotite, garnet-biotite-schist, hornblende schist, calc-silicate schist, marble, and quartzite. Closer to the coast the lithologies are primarily Cretaceous to Jurassic greywacke and mudstones with minor andesitic to basaltic volcanic rocks and limestone.

2.2. Climate

Climate of KB is maritime and moderated by the North Pacific Ocean. Yearly precipitation in Homer, Alaska (see Figure 1b) averages 635 mm/yr and temperature averages 3.3°C. Between 1949 and 2020 mean winter temperatures in Homer have increased 5.5°C while mean summer temperatures increased 2.3°C (values converted from Alaska Climate Research Center, 2022). Precipitation peaks in September and October with lowest precipitation occurring in June and July and due to its geographic location, KB receives less precipitation than expected in a maritime climate due to the rain shadow from the Kenai Mountains. Generally, the south side of KB receives more precipitation than the north side. For example, the village of Seldovia is located on the southwest part of KB and on average receives 900 mm/yr of precipitation and has an average temperature of 4.5°C.

The LC study region near Juneau AK also has a maritime climate with mild winters and cool, wet summers. Average temperature recorded at the Juneau airport is 5.6°C and mean annual precipitation is 1,580 mm/yr and is highest in early fall and lowest during spring. During the twentieth century, temperatures in the Juneau area have risen 2°C, largely driven by increased winter temperatures. In the last 60 years winter temperatures in Juneau increased by approximately 1.5°C. Winter snowfall declined and total winter precipitation including rain and snow increased ~10 mm (Kelly et al., 2007).

2.3. Watershed Characteristics

The watersheds included in this study with percent glacier cover noted at KB are Grewingk (62%), Wosnesenski (28%), Halibut (16%), Tutka (8%), and Jakolof (0%) (Table 1, Figure 1) and the LC watersheds are Mendenhall

Table 1
Watershed Characteristics for the Kachemak Bay and Lynn Canal Study Regions

	Kachemak Bay					Lynn Canal				
	Grewingk	Wosnesenski	Halibut	Tutka	Jakolof	Mendenhall	Herbert	Lemon	Cowee	Sheep
Area (km^2)	108	248	55	64	19	222	152	61	110	15
Glacier area (km^2)	67	69	9	5	0	123	64	15	13	0
% Glacier	62	28	16	8	0	55	42	25	12	0
Discharge (m^3/s)	38	38	6	10	0.57	55	31	7	11	2.8
Specific discharge (mm/hr)	1.28	0.54	0.42	0.58	0.11	0.89	0.75	0.43	0.36	0.68
Seasonal triangle type	1a	2	2	2	3a	1b	2	2	2	3b
Max. elevation (m)	1,641	1,569	1,494	1,275	1,140	2,013	2,120	1,676	1,765	1,288
Mean elevation (m)	793	648	725	625	502	994	860	804	648	559
Mean aspect	213	190	189	178	162	200	196	196	204	195
Mean slope	14	20	26	45	21	18	18	22	23	29
% Vegetation	14	44	51	46	93	25	43	58	77	92
% Forest	2	18	7	18	64	10	30	25	58	13
% Shrubland	12	25	45	28	29	15	13	32	19	79
% Herbaceous	0	1	0	1	0	0	0	0	0	0
% Barren land	13	22	23	37	4	11	9	13	8	5
% Lake	4	1	0	0	0	2	1	0	0	0
% Wetland	2	5	1	2	2	1	5	1	5	1

(55%), Herbert (42%), Lemon (25%), Cowee (12%), and Sheep (<2%) (Table 1, Figure 1). These watersheds were chosen primarily because they span a gradient of highly glacierized to non-glacierized catchments and because of the relative ease of access in the generally rugged mountainous region. Detailed descriptions of watershed characteristics and the geology of each region are found in Text S1 in Supporting Information S1.

3. Methods

3.1. Watershed Analysis

Watershed boundaries originated from the USGS Watershed Boundary Dataset mapped using the 12-digit hydrologic unit code. Glacier coverages for KB were delineated using Sentinal-2 imagery taken during September 2018. After ingesting images into GIS, glacial extents were mapped using manual and supervised classification techniques. The Randolph Glacial Inventory 6.0 (https://www.glims.org/RGI/) was used for the glacier extents for the LC study sites. Watershed elevation statistics were extracted from 5 m digital terrain model, produced by the USGS Alaska Mapping initiative. Vegetation coverage areas originated from the USGS National Land Cover Database. Calculations for wetland and lake coverage were based on data from the U.S. Fish & Wildlife Service National Wetlands Inventory (https://www.fws.gov/wetlands/) using any body designated as palustrine, or riverine.

3.2. Climate Analysis

To provide a robust analysis of the climate record for each study region we calculated the 30-year averages of temperature and precipitation using DAYMET V4.0 (Thornton et al., 2022). Additionally, we calculated climate averages for the study period, 2019–2021. The DAYMET dataset was accessed and analyzed via Google Earth Engine. For each region the gridded DAYMET dataset was clipped to the study region using the geometries of two of the 10-digit HUCs that cover the region. The mean and standard deviation of precipitation and air temperature was calculated using native Google Earth Engine JavaScript functions.

3.3. Field Measurements

Monthly grab samples of stream water were taken at each of the KB and LC study streams between April and October 2019 to 2021, with additional sampling visits in March 2019, and 2021 and January 2021 at the KB sites.

At KB a hand held YSI ProDSS was used to measure stream water temperature, specific conductance, and pH at the time of each stream water grab sample. At the LC sites pH was measured using an Orion Star A221 portable pH meter.

Dataloggers were installed at each of the selected sites for long-term data collection (Figure 1). At each site, a 4-inch PVC tube open at the bottom attached to rebar/fence posts (KB) or metal pipe housing secured to the stream bed (LC) was used as a protective casing for the stream sensors. Stream height, conductivity, and temperature were measured in each stream typically between March through October. Dataloggers were Onset Computer Corporation HOBO Water Level Data Logger (U20L-04, ±3%), Fresh Water Conductivity Data Logger (U24-001, drift 3% yr^{-1}), and water temperature was taken from the conductivity data logger. Stream water conductivity was converted to specific conductance using HOBOware Pro Conductivity Assistant. In the LC sites, YSI sondes were used to measure temperature and specific conductance. At the KB sites, a separate pressure transducer was deployed near the stream, attached to a tree for recording barometric pressure in order to correct for atmospheric pressure and calculate stream height. Sensors were set to record data at 15-min intervals.

Monthly discharge measurements were made at each stream from April to October in both regions. In KB, manual discharge measurements were made when streams were wadable at lower flow conditions using a Marsh McBirney Flo-Mate 2000 or an Ott MF-Pro. A SonTek M9 or S5 Acoustic Doppler Current Profiler (ADCP) was employed during periods of high flow and was used in all measurements at Grewingk Stream. Rating curves were created using stream height, monthly, and high frequency discharge measurements. Discharge for all 3 years at the Wosnesenski River was derived from modeled data originating from the work of Beamer et al. (2016) (Nash Sutfcliffe Efficiency values of 0.85–0.91) because this stream is highly braided and meandering making manual measurements insufficient. Similarly, due to high flow events causing lost equipment at Halibut, we use the modeled data for 2021 discharge and 2020 discharge for Tutka. For LC sites, discharge in Lemon Creek (#15052000) and Mendenhall River (#15054200) were measured by the U.S. Geologic Survey. In the other LC streams, stage height was measured at 15-min intervals using a stilling well equipped with a pressure transducer (In-Situ Troll) or a Campbell Scientific SR50 A sensor (Herbert River). Stage measurements were converted to flow with a rating curve developed from manual measurements of discharge made using a FlowTracker at wadable levels and a River Ray ADCP at high flows.

In KB we collected snow, ice, and rain samples for water stable isotope analysis. Snow was collected on the Wosnesenski Glacier. In January 2021, we collected fresh snow samples at 1,000 m and 500 m and a snow pit dug at 1,000 m on the divide between the Grewingk and Halibut watersheds. The snow pit was dug to the ground and was 180 cm in depth, samples were taken every 20 cm. Rain samples were collected in Palmex RS1 Rain Samplers installed in Grewingk and Wosnesenski watersheds near the main gage sites with another RS1 installed at sea level near the Jakolof watershed. Ice samples were collected directly from the Wosnesenski, Doroshin, and Grewingk Glaciers. We also collected numerous ice samples from glacier icebergs floating in the proglacial Grewingk Lake. Similar samples were collected in the LC sites and the sources are described in Section 4.

3.4. Geochemical Analysis

Water samples were taken from each of the studied streams at monthly intervals. Water was collected in 1-L high density polyethylene (HDPE) bottles. Sample bottles were rinsed three times with sample water prior to containing the sample. Samples for major elemental analysis were filtered with 0.45 μm filters with PTFE membranes. Water samples for DOC analysis were filtered through combusted Whatman GF/F filter (0.7 μm). All samples were kept refrigerated until analysis. TSS was determined by filtration of known sample volume onto a precombusted and pre-weighed Whatman GF/F filter (0.7 μm). Filters were then dried at 60°C overnight and reweighed to calculate sediment concentration.

Water samples were analyzed for δ^2H and $\delta^{18}O$ using a Picarro L-1102i WS-CRDS analyzer (Picarro, Sunnyvale, CA) in the ENRI Stable Isotope Laboratory at the University of Alaska Anchorage. International reference standards (IAEA, Vienna, Austria) were used to calibrate the instrument to the VSMOW-VSLAP scale and working standards (USGS45: $\delta^2H = -10.3‰$, $\delta^{18}O = -2.24‰$ and USGS46: $\delta^2H = -235.8‰$, $\delta^{18}O = -29.8‰$) were used with each analytical run to correct for instrumental drift. Long-term mean and standard deviation records of a purified water laboratory internal QA/QC standard ($\delta^2H = -149.80‰$, $\delta^{18}O = -19.68‰$) yield an instrumental precision of 0.93‰ for δ^2H and 0.08‰ for $\delta^{18}O$.

Sample analysis for alkalinity and major elements (Ca, Mg, Na, K, Si, Cl^-, SO_4^{2-}) was performed at SGS Environmental Services in Lakefield Ontario. Alkalinity, for samples taken during the 2019–2020 seasons, was analyzed by titration using reference method SM 2320. Alkalinity was measured in the field using Chemtrics Titrets 10–100 ppm total alkalinity kits, during the 2021 field season (KB sites only). Anions were analyzed by ion chromatography following the methods in EPA300/MA300-inos1.3. Inductively coupled plasma mass spectrometry (ICP-MS) was used for elemental analysis using the methods SM 3030/EPA 200.8. All elemental analytical error was reported to be less than 10%. The concentrations were calculated using Geochemist's Workbench Community Edition 15.0 based on the alkalinity, and pH of each sample. For the purpose of this study we report the sum of Ca, Mg, K, Na, HCO_3^-, SO_4^{2-}, Cl^-, and SiO_2 as TDS in units of mg/L.

The DOC samples were analyzed with a Shimadzu Total Organic Carbon Analyzer (TOC-L-CSH). Samples were acidified with HCl and sparged to remove inorganic carbon followed by high-temperature combustion. DOC (measured as non-purgeable organic carbon) were reported as the average value of three to five replicate injections from each sample. POC and $\delta^{13}C_{POC}$ samples were analyzed using the same filters used to obtain sediment concentrations. Carbonates were removed from POC samples by triple sulfurous acid and analyzed at the UC Davis Stable Isotope Facility utilizing a Micro Cube elemental analyzer (Elementar Analysensysteme GmbH, Hanau, Germany) interfaced to a PDZ Europa 20-20 IRMS (Sercon Ltd., Cheshire, UK). POC concentrations were calculated by dividing the total mass of C by the volume of water filtered.

3.5. Yields of Dissolved and Suspended Riverine Matter

For this study, we use the instantaneous discharge measurements for the calculation of yields. When instantaneous discharge values were not available we used daily average discharge values. Modeled daily discharge values, based on Beamer et al. (2016), were used for all yield calculations for the Wosnesenski, the 2021 season at Halibut, and the 2020 season at Tutka. The yields of TDS, DOC, POC, and TSS were calculated by multiplying the concentration by the instantaneous (or daily averaged) discharge measurement and dividing by the watershed area.

Discharge and in-situ specific conductance data were averaged across the 3 years of collection for each stream site and are presented as averaged daily values. At Lemon Creek, the conductivity logger was lost on several occasions, leading to gaps within the dataset. Solute, $\delta^{13}C_{POC}$, and sediment data were grouped by sample month and averaged and the resulting plots of solutes, sediment, and $\delta^{13}C_{POC}$ illustrate 3 years of collected data averaged together for the specified month. Additionally, we ran a two sample Kolmogorov-Smirnov test to explore the contrasts in solute distributions between each study region.

4. Results

4.1. Hydroclimate and Hydrology

Seasonal average precipitation, air temperature, and specific discharge of the 10 study sites indicate strong seasonal cycles in hydroclimate and water yields over the 3 years of record (Figure 2). Within both KB and LC regions, precipitation was greatest during late summer and fall. During spring and early summer, precipitation was at a minimum in KB. In LC spring and early summer precipitation was elevated compared to KB.

During the 3 years of observations in KB there were large fall rain events, which dominated the monthly averages of precipitation. Overall, there are less days with measurable precipitation at KB compared to LC. This can be observed within the hydrographs, with LC streams showing multiple precipitation induced peaks in runoff during the late summer and early fall. Conversely, the hydrographs for the KB streams show fewer peaks in runoff during late summer and early fall.

There are similar seasonal patterns in runoff between KB and LC streams such that seasonal hydrographs of the glacierized catchments show an increase in discharge from May through July, primarily from snow and glacier ice contributions punctuated by rainfall. After the cessation of seasonal snowmelt, specific discharge decreases until fall precipitation events cause pronounced peaks in the hydrographs. The non-glacierized watershed seasonal hydrographs display an increase in flow in spring, then a slow decline through the summer as snow cover is lost and evapotranspiration increases. Jakolof stream, in KB would intermittently lack surface flow during July–

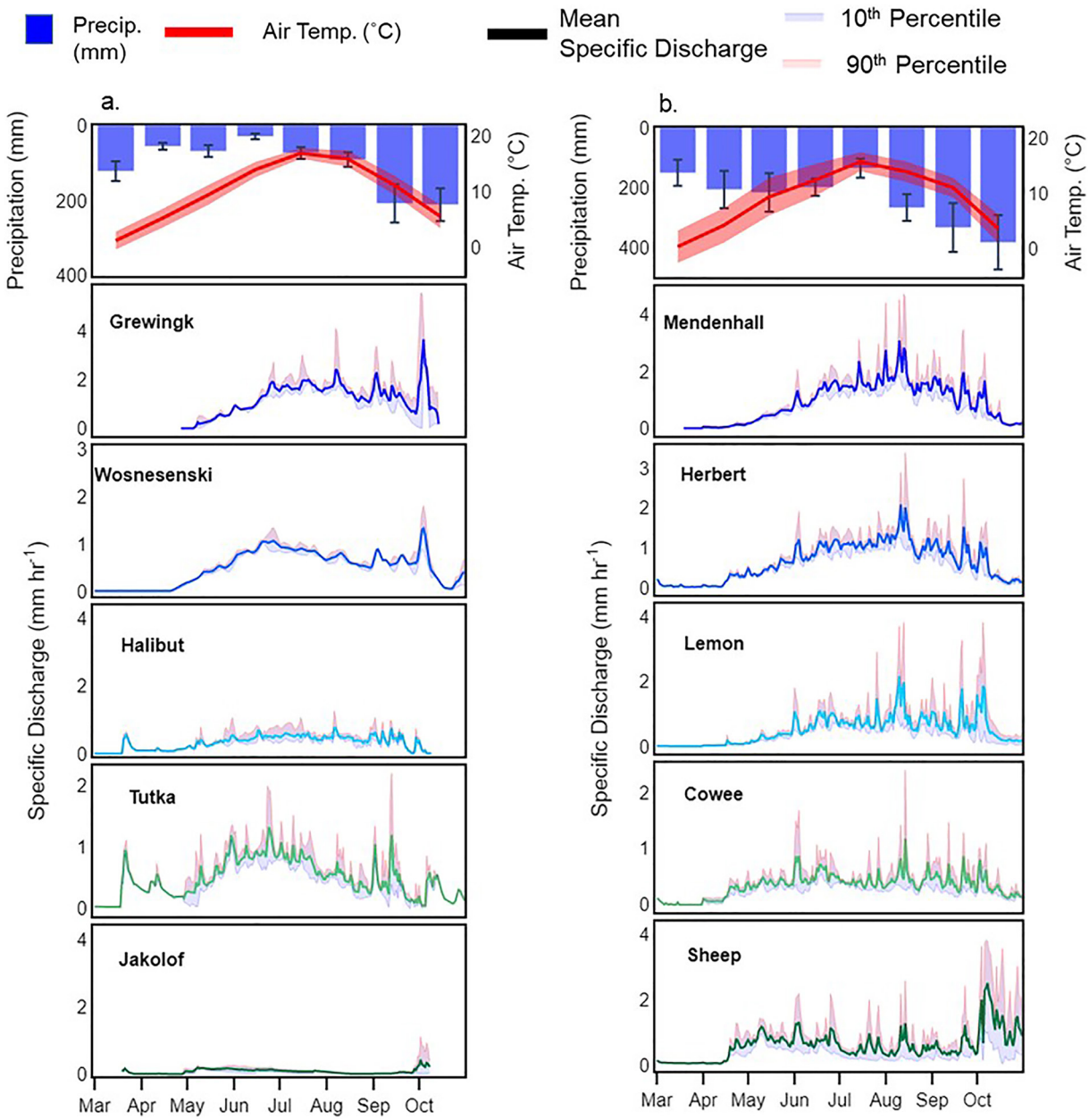

Figure 2. Seasonal precipitation, air temperature, and hydrographs for KB (a) and LC (b) study sites. Precipitation and air temperature are averages from 2019 to 2021 acquired from DAYMET V4. Seasonal runoff is averaged across the 3 years of data collection with the 90th (red) and 10th (blue) percentiles shown.

September. The glacierized catchments in both regions generally had the highest specific discharge with the exception of Sheep, which had a high specific discharge compared to Cowee (Table 1).

4.2. Specific Conductance and $\delta^{18}O$

Changes in the specific conductance and $\delta^{18}O$ can be used as an indicator of how sources of water to the streams change seasonally within and across the two study regions. Overall KB streams averaged higher specific conductance compared to LC streams. Within the glacierized catchments of KB and LC specific conductance decreased in the spring, remained consistently low in the summer, and rose in August (KB) and September (LC) (Figures 3a and 3b, Figure S2 in Supporting Information S1). Specific conductance in the non-glacierized streams remained relatively stable throughout the seasons with lower values associated with rain events.

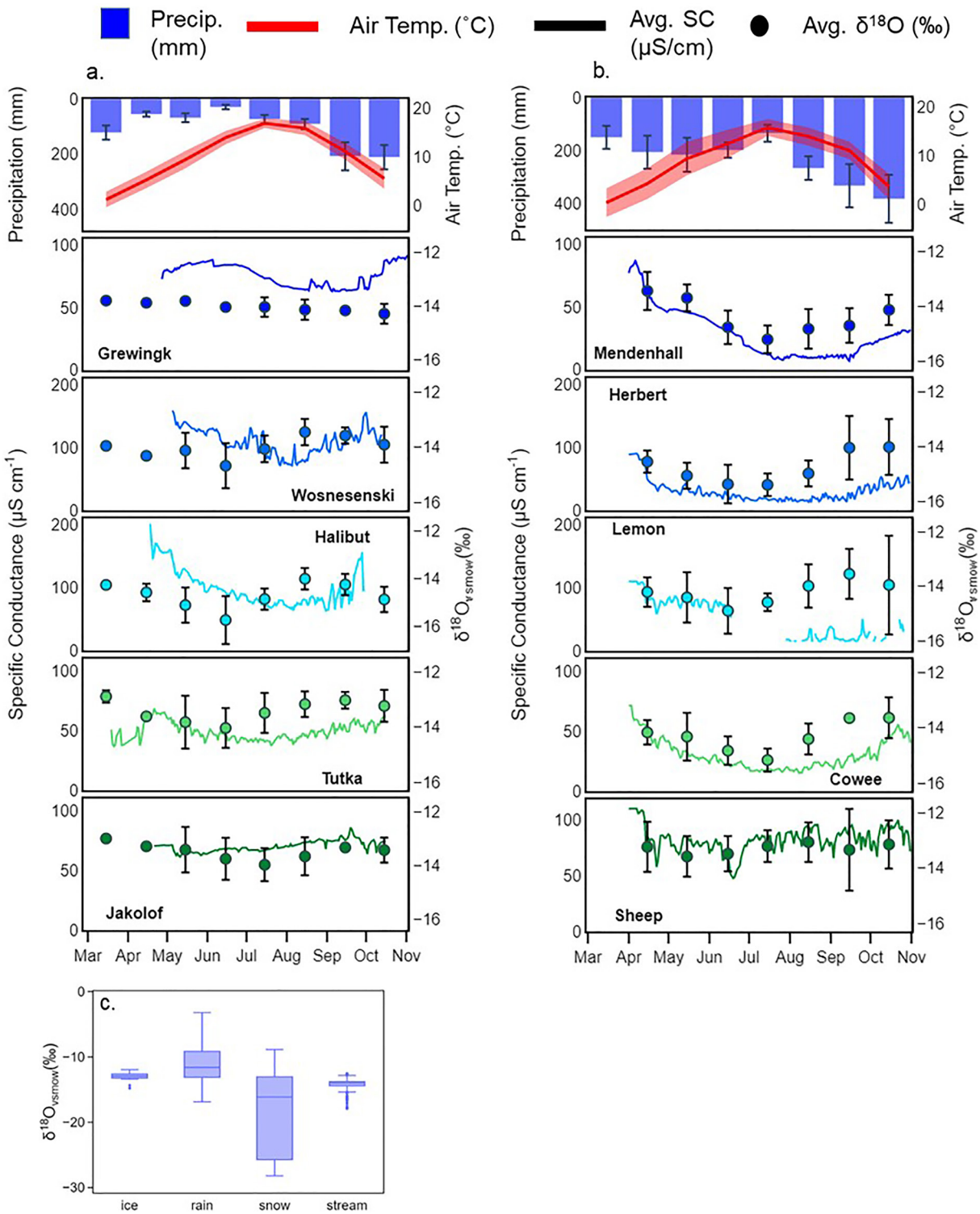

Figure 3. Seasonal variability of precipitation, air temperature, and stream specific conductance and $\delta^{18}O$ for KB streams (a) and LC streams (b). Precipitation and air temperature are averages from 2019 to 2021 acquired from DAYMET V4. Panel (c) is the $\delta^{18}O$ values for ice, rain, snow, and average stream values for the KB study region.

Stream water $\delta^{18}O$ values in the glacier fed streams in KB, with the exception of Grewingk, had mean $\delta^{18}O$ values that were the most depleted in June (Figure 3a). Stream $\delta^{18}O$ values at Grewingk had extremely low variability ranging from −14.27‰ to −13.80‰. Average stream water δD and $\delta^{18}O$ for KB and LC fall close the Global

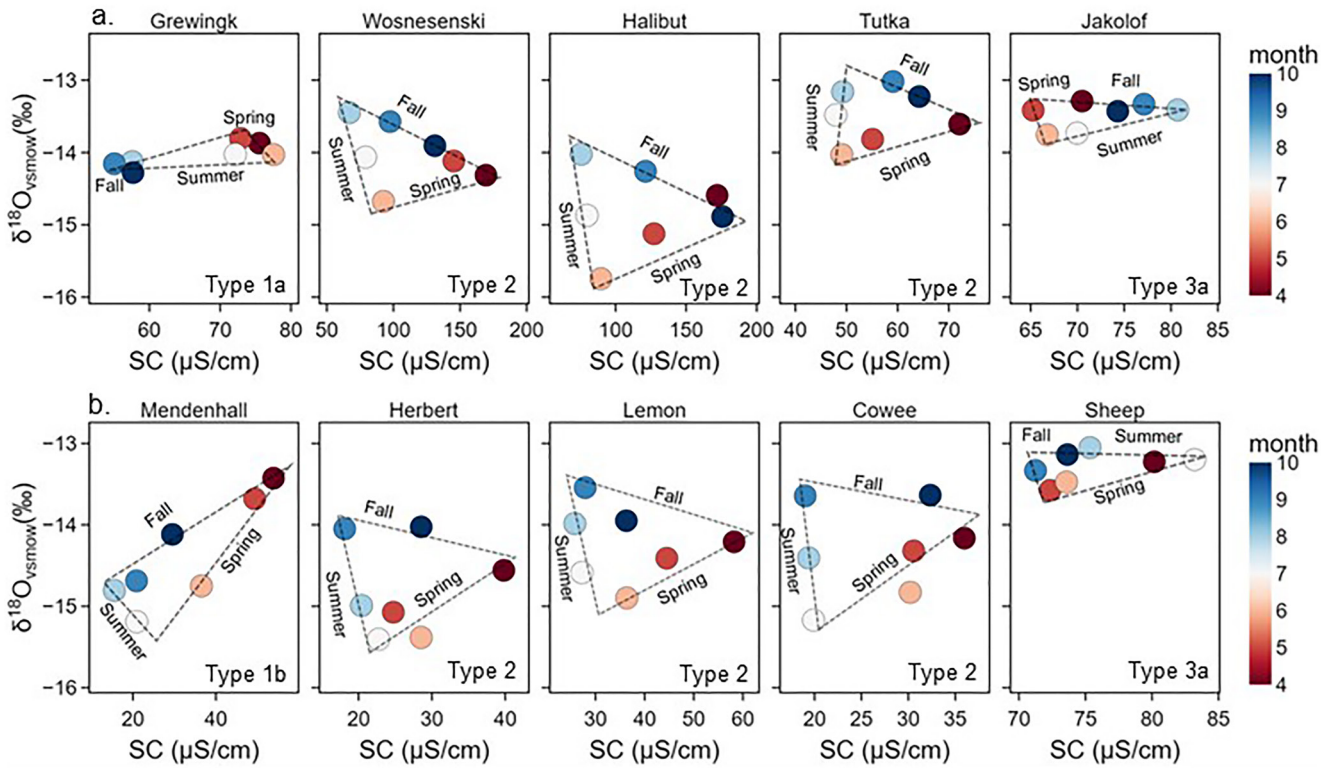

Figure 4. Seasonal variability in $\delta^{18}O$ and specific conductance of stream samples in Kachemak Bay (a) and Lynn Canal (b). Triangles are drawn and annotated to generalize the seasonal patterns in the two variables. Seasons are defined by the meteorological seasons.

Meteoric Water Line (GMWL; Figures S1a and S1b in Supporting Information S1). Mean stream water $\delta^{18}O$ in KB streams ranged from −13.07‰ in Tutka to −14.40‰ in Halibut. In LC streams, $\delta^{18}O$ values ranged from −12.53‰ in Sheep Creek to −14.47‰ in Herbert (Figure S1b in Supporting Information S1). Herbert (LC) and Halibut (KB) stream waters had the most depleted isotope values of the LC and KB sites. Cowee Creek (12% glacier coverage) isotopic values were more depleted compared to Mendenhall River and Lemon Creek. At KB, Tutka on average was more enriched compared to non-glacierized Jakolof Creek. In the KB streams, the greatest year to year variability in $\delta^{18}O$ values, illustrated by error bars in Figures 3a and 3b, was observed in the spring and early summer, with the least variability occurring in the fall (Figure 3a). Contrastingly, LC streams had the greatest variability in $\delta^{18}O$ values during the fall, with limited variability in the summer months (Figure 3b).

Between the two regions the stable water isotope values of rain and stream water are similar while snow and ice values are more depleted in the LC region. For reference Figure 3c (see also Figure S3 and Figure S4 in Supporting Information S1) illustrates the $\delta^{18}O$ values for the primary water sources contributing to stream flow including snow, rain, and ice within the KB region. Snow ($\mu = -18.83‰$) had the greatest variability in $\delta^{18}O$ followed by rain ($\mu = -11.02‰$). Stream isotopic values of $\delta^{18}O$ across all KB streams range from −12.96‰ to −17.88‰ ($\mu = -14.01‰$). The $\delta^{18}O$ values for ice samples taken from Grewingk Glacier and the Doroshin Glacier in the Wosnesenski watershed (see Figure 1) range from −11.95‰ to −14.76‰ ($\mu = -12.99‰$). In the LC region rain, snow, and ice $\delta^{18}O$ values average −11.4‰ (Fellman et al., 2014), −16.8‰ (Fellman, Hood, Raymond, et al., 2015), and −16.7‰ (unpublished), respectively. Stream water $\delta^{18}O$ values averaged −14.22‰ in the LC sites.

We further contextualize the seasonal changes in sources of water to streams as defined in specific conductance and $\delta^{18}O$ space using a "seasonal triangle" classification scheme. Here we define three primary and four subtypes of seasonal relationships we observed between specific conductance and $\delta^{18}O$ (see Figure 4). Type 1 comprise the streams with proglacial lakes with two subtypes 1a and 1b. Type 1a are defined by limited seasonal variability in $\delta^{18}O$ with a decrease in specific conductance in the late summer and fall. Type 1b are defined by a decrease in specific conductance and depletion in $\delta^{18}O$ values from spring to summer and an increase in specific conductance

Table 2
Summary of Average Concentrations of Dissolved, Suspended Matter, and $\delta^{13}C_{poc}$ Across the Two Study Regions

	TDS (mg/L)	σ	DOC (mg/L)	σ	TSS (mg/L)	σ	POC (mg/L)	σ	$\delta^{13}C_{vpdb}$ (‰)	σ
Kachemak Bay										
Grewingk (62%)	46.3	11.1	0.336	0.130	54.87	27.77	0.156	0.060	−28.331	0.745
Wosnesenski (28%)	75.5	28.8	0.417	0.146	138.51	314.22	0.259	0.292	−28.822	1.776
Halibut (16%)	85.7	30.7	0.460	0.195	92.51	218.39	0.215	0.535	−29.134	1.686
Tutka (8%)	39.9	6.4	0.375	0.115	15.27	33.96	0.049	0.032	−29.146	1.305
Jakolof (0%)	51.7	9.5	0.947	0.345	0.82	0.87	0.064	0.048	−29.992	1.928
Lynn Canal										
Mendenhall (55%)	21.7	10.2	0.494	0.215	76.00	67.02	0.096	0.029	−26.645	1.012
Herbert (42%)	17.3	5.9	1.109	0.802	228.78	257.86	0.213	0.150	−24.596	2.133
Lemon (25%)	24.9	7.2	0.680	0.392	79.23	107.18	0.290	0.356	−25.552	1.527
Cowee (12%)	17.3	6.3	1.706	1.075	14.96	24.50	0.191	0.102	−27.568	0.586
Sheep (0%)	49.8	11.4	0.646	0.346	6.72	6.07	0.304	0.254	−27.809	0.786

Note. Percent of glacier coverage is shown in parentheses next to watershed name.

and $\delta^{18}O$ values from summer to fall. Type 2 relationships comprise all other glacierized streams from across both regions. Type 2 are defined by decrease in specific conductance and $\delta^{18}O$ from spring to summer. In the summer $\delta^{18}O$ values become enriched and specific conductance values continue to decrease. In the transition from summer to fall the specific conductance increases while the $\delta^{18}O$ values become depleted. Type 3 comprise the non-glacierized streams and we define two subtypes 3a and 3b. Type 3a relationships have little seasonal variability and a counterclockwise relationship in specific conductance and $\delta^{18}O$ from spring to fall. Type 3b also has little variability in $\delta^{18}O$ but has a distinctive peak in specific conductance in the spring and summer making it different from the other streams where we generally observed the highest specific conductance values in fall and spring.

4.3. Concentrations of Dissolved Components

This and the next three sections of results are focused on the concentrations and yields of geochemical components measured in all streams. The comparisons within and between study regions are made using averages in Tables 2 and 3 that are complimentary to data presentation in Figures 5–8(see also Figure S5 in Supporting Information S1). Overall the results indicate that concentrations and yields of geochemical components are distinct between the KB and LC regions. First, we observe that the inorganic fraction of the dissolved load is higher in the KB streams while the organic carbon fraction is elevated in LC streams. Second, we found that solute and suspended yields peak in early summer in KB streams while peak yields were shifted in LC to late summer and fall.

The contrasting geochemistry between the KB and LC streams is illustrated in Table 2 and Figures 5a–5d. There were large differences in the distributions (significantly different at the $p < 0.05$ level of a Kolmogorov-Smirnov test) in water chemistry between the KB and LC catchments such that KB streams had higher average TDS and greater ranges in concentrations. The seasonal variation of TDS in KB and LC glacierized streams was similar, with higher concentrations in spring and fall and lower concentrations mid-summer (Figures 5a and 5b). Non-glacierized Jakolof in KB had TDS variability similar to the glacierized streams. The non-glacierized endmember in LC, Sheep Creek, had the highest TDS concentrations and disparate seasonal variability to the glacierized catchments. Average concentrations of DOC were consistently lower in KB streams (Table 2), however, the seasonal variation of DOC observed in KB and LC streams was similar with spring and fall having the highest concentrations and the lowest during the summer months (Figures 5c and 5d).

4.4. Suspended Matter

We observed distinct seasonal variations in the suspended matter across the KB and LC streams (Table 2 and Figure 6). KB streams generally had TSS concentrations that increased between spring and summer and declined

Table 3
Summary of Average Yields of Dissolved and Suspended Matter Across the Study Regions

	TDS (kg/km^2/d)	σ	DOC (kg/km^2/d)	σ	TSS (kg/km^2/d)	σ	POC (kg/km^2/d)	σ
Kachemak Bay								
Grewingk (62%)	1,105.5	1,036.5	9.52	11.38	1,522	1,300	4.14	3.48
Wosnesenski (28%)	845.4	603.3	5.30	5.16	3,041	6,926	5.39	7.82
Halibut (16%)	542.0	442.9	4.38	8.10	2,197	5,632	6.40	22.38
Tutka (8%)	422.7	302.2	4.24	4.40	417	1,257	0.79	1.30
Jakolof (0%)	177.7	175.1	3.97	5.18	2	3	0.15	0.16
Lynn Canal								
Mendenhall (55%)	492.9	421.5	11.03	9.50	2,510	3,186	2.67	2.09
Herbert (42%)	332.9	239.1	17.70	15.41	6,877	10,944	5.60	7.65
Lemon (25%)	432.3	460.9	11.51	15.52	2,478	5,209	4.11	4.31
Cowee (12%)	205.9	109.7	17.95	13.17	176	207	2.20	1.34
Sheep (0%)	754.8	466.8	9.87	6.96	125	136	4.90	5.03

Note. Percent of glacier coverage is shown in parentheses next to watershed name.

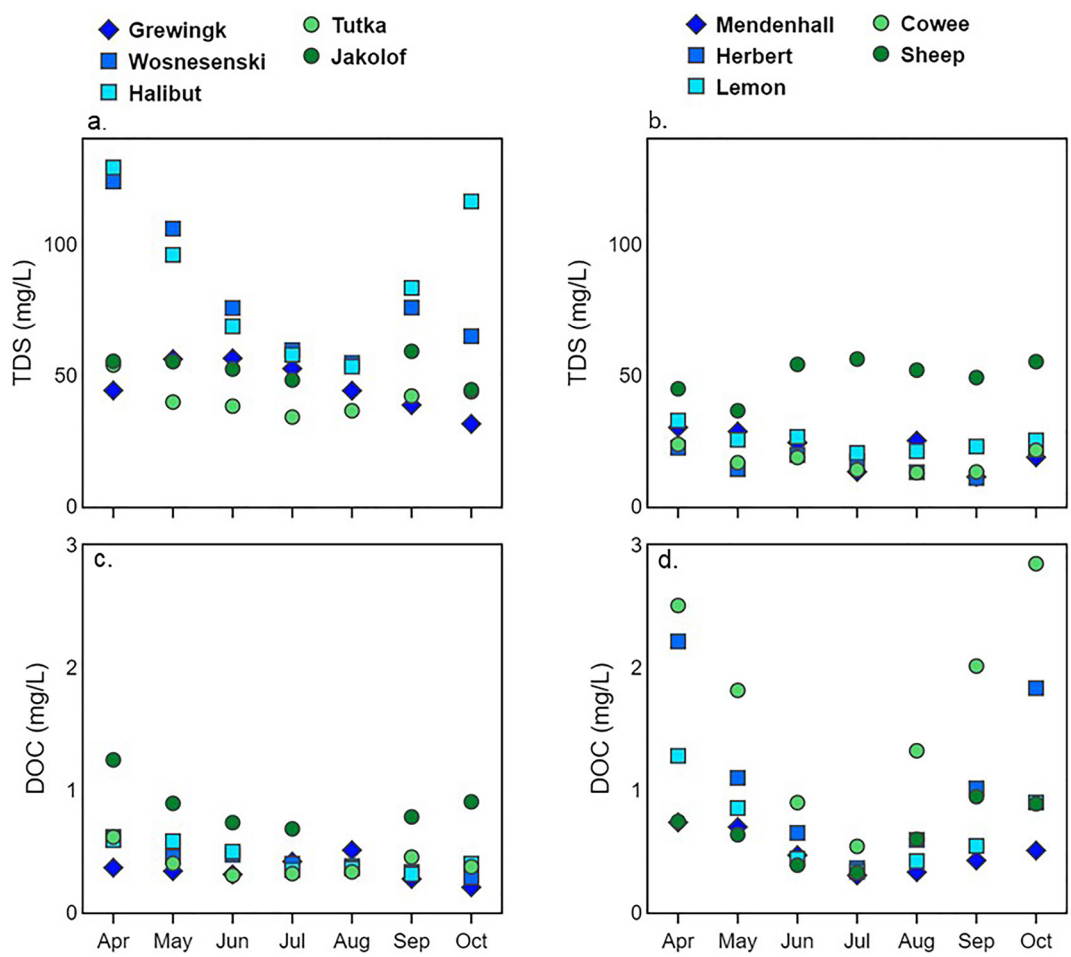

Figure 5. Seasonal concentrations variability of TDS and DOC. The left panel presents KB data and the left shows LC data. Each point represents the average value for 3 years of data collected during the specified month.

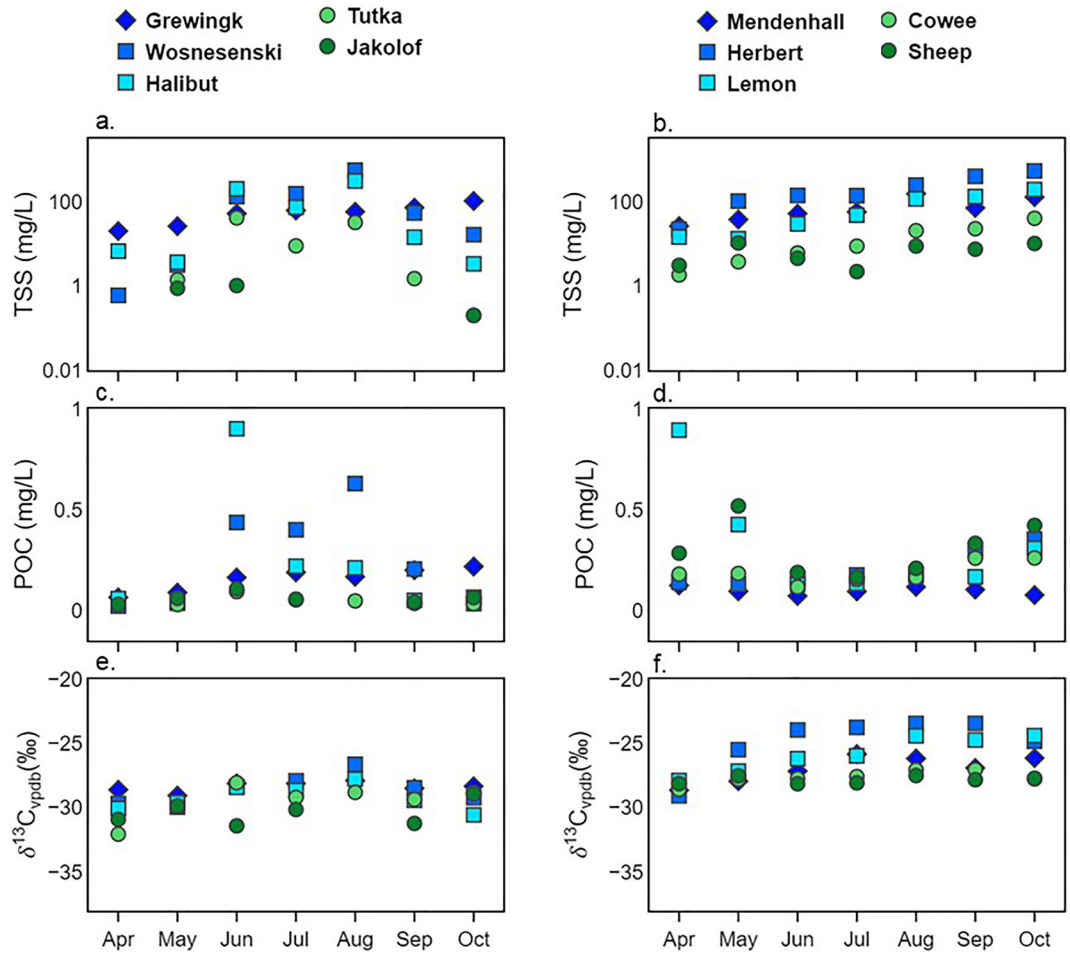

Figure 6. Seasonal variability of TSS, POC, and $\delta^{13}C$. The left panel presents KB data and the left shows LC data. Each point represents the average value for 3 years of data collected during the specified month.

into the fall in contrast to LC, where the TSS concentrations were at a minimum in spring and climbed steadily into October. Across both regions, heavily glacierized catchments had elevated TSS compared to watersheds with less glacier or no glacier coverage. POC concentrations in the glacierized streams at KB tended to have elevated concentrations in the late spring and early summer. LC stream POC concentrations were elevated in the spring and fall and at the lowest in June and July. The $\delta^{13}C_{POC}$ values in KB streams were more depleted compared to LC (Table 2 and Figures 6e and 6f) and seasonal changes in the $\delta^{13}C_{POC}$ at KB were subtle with a slight enrichment observed in August. The LC streams, with the exception of Mendenhall, beginning in June through October had an enrichment of $\delta^{13}C_{POC}$ values, though the observed enrichment in Cowee and Sheep was minimal.

4.5. Yields of Dissolved Components

In KB the glacierized streams had the highest average yields of TDS and DOC (Table 3) but in the LC streams the moderate to high glacier cover watersheds had elevated TDS yields compared to low glacier coverage Cowee. Interestingly, we observed the highest TDS yields in non-glacierized Sheep Creek. DOC yields were the highest in the glacierized watersheds within LC with Herbert and Cowee having the highest in the study region.

Timing of the yields of TDS and DOC (Figure 7 and Table 3) have dissimilar seasonal peak variability between the two study regions such that in KB the observed peak yields occurred in July and declined into the fall within the glacierized catchments whereas in the majority of LC streams the peaks were in August and September, with Sheep Creek at maximum in June. Generally, the DOC yields in KB are highest in June to July, with Grewingk as an outlier having the greatest DOC yields in August. DOC yields declined in KB through October to reach similar

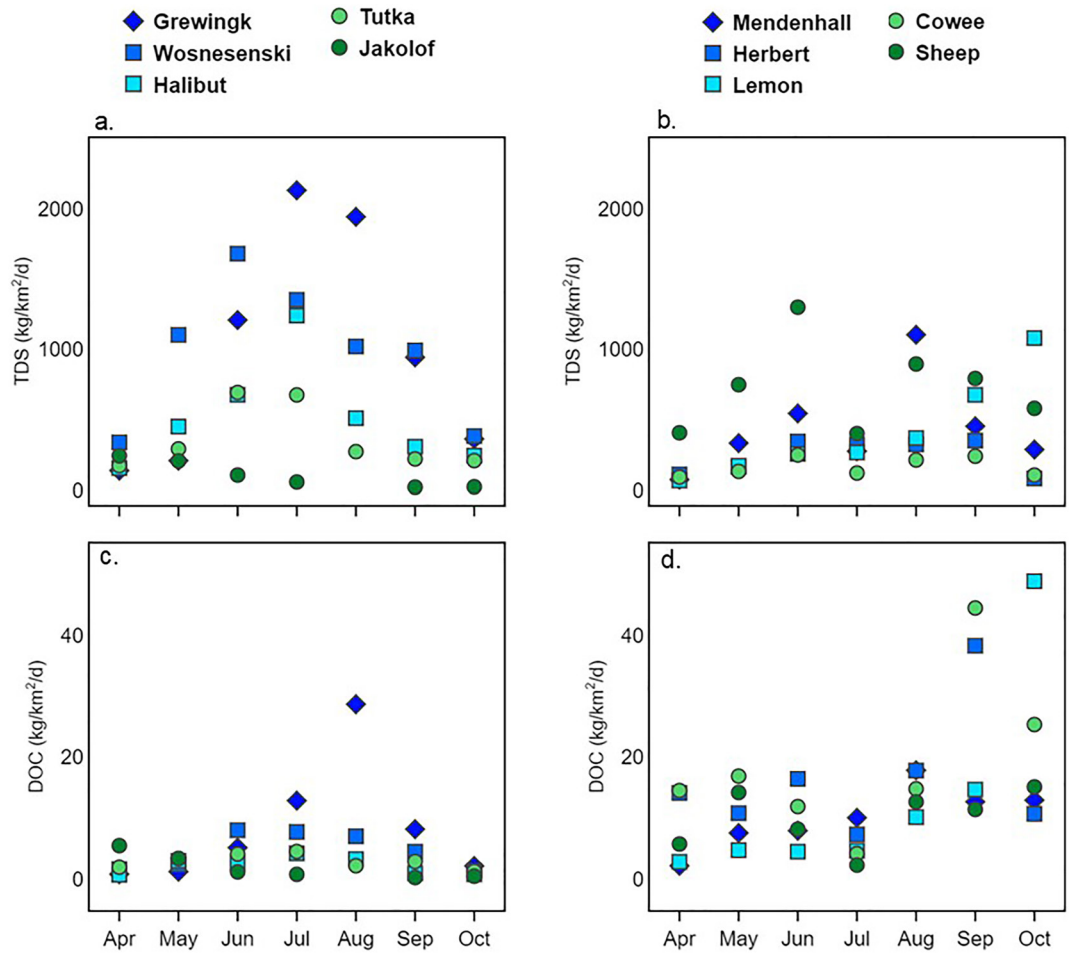

Figure 7. Seasonal variability of the yields of TDS and DOC. The left panel presents KB data and the left shows LC data. Each point represents the average value for 3 years of data collected during the specified month.

values observed during the spring. In the LC streams, broadly, the DOC yields are high in the spring and declined through July then peaked in late summer and into the fall months.

4.6. Yields of Suspended Matter

The TSS yields were greater in LC streams compared to KB. In KB the TSS yields peaked in August within Grewingk, Wosnesenskai, and Halibut, while the minimally glacierized Tutka had peak TSS yields in June (Figure 8a). In LC streams TSS yields, with the exception of Sheep, continually increased from spring until fall. Yields of POC, in KB streams peaked in August; however, Tutka and Jakolof had extremely limited seasonal variability with no discernible peak yields (Figure 8c). In LC, Mendenhall, and Lemon POC yields increased through September and in Mendenhall decreased in October, but at Lemon there was a sharp increase in POC yields in October (Figure 8d). Herbert POC yields steadily increased into August and sharply increased in September and October. POC yields in Cowee are steady from April to July and slightly increase in August through September with a small decrease in October.

5. Discussion

5.1. Regional Variability in Hydroclimate-Driven Seasonal Water Sources and Yields

Analysis of seasonal hydrographs and specific conductance from the 10 GoA streams reveal common trends across the KB and LC hydroclimate regions. The presence of moderate to heavy glacier cover within a watershed

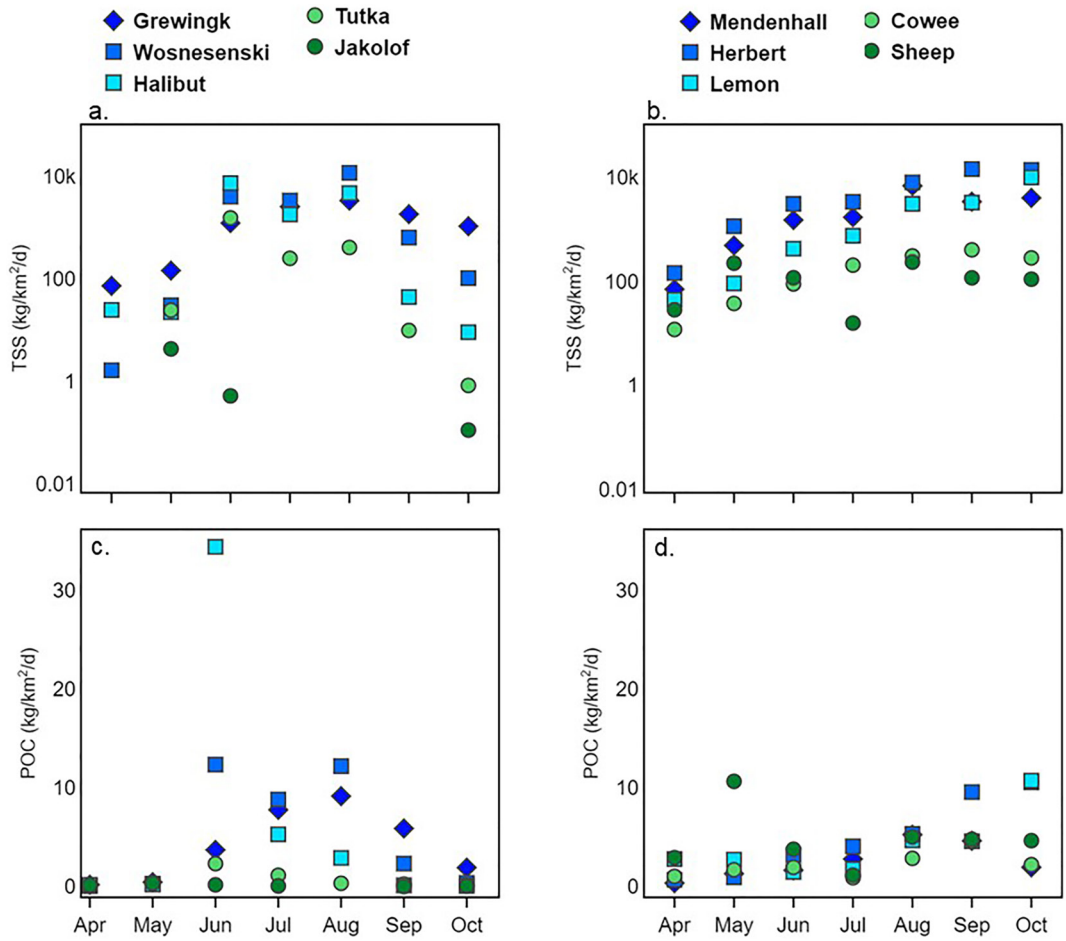

Figure 8. Seasonal variability of TSS and POC yields. The left panel presents KB data and the left shows LC data. Each point represents the average value for 3 years of data collected during the specified month.

invariably controls the timing and flux of freshwater. Generally, the specific discharge in heavily glacierized watersheds was greater than those of non-glacierized watersheds, which is consistent with other temperate glacierized watersheds (e.g., Fleming, 2005). Based on regional glacier mass balance studies and modeling, most of the glaciers within the KB and LC region are losing mass leading to increased freshwater yields to coastal environments (Deb et al., 2015; Larsen et al., 2015; Neal et al., 2010; Radić et al., 2014; Valentin et al., 2018; Yang et al., 2020; Young et al., 2021). As glaciers recede different runoff regimes will emerge altering the timing of freshwater inputs. However, due to differences in hydroclimate (i.e., KB and LC), runoff regimes across the GoA may show contrasting responses to future glacier recession.

A major difference between LC and KB hydrographs is that the LC streams have continuously high seasonal discharge, primarily sustained by rain, whereas the KB streams decline in overall discharge but respond with sharp peaks to event driven rain. The high specific conductance in LC streams occurs during spring baseflow conditions, before the onset of the melt season. Stream water subsequently becomes very dilute from snowmelt and glacier melt in the late spring and early summer and, distinctive to KB streams, remains relatively dilute into the fall likely driven by large consistent amounts of rain. The predicted increase in fall rains (Beamer et al., 2017) and diminished snow pack is expected to alter the timing of discharge such that KB streams may eventually have similar seasonal hydrographs to those of the present-day LC streams. This affect may be attenuated due the geographic position of KB, in that it is situated in the rain shadow of the Kenai Mountains. However, future freshwater yields to the GoA will be altered due to the evolution and intensification of the hydroclimate. This change in the timing of freshwater flux will also affect the timing and fluxes of micronutrients and sediment transferred to the intertidal and coastal ecosystems (Figure 9).

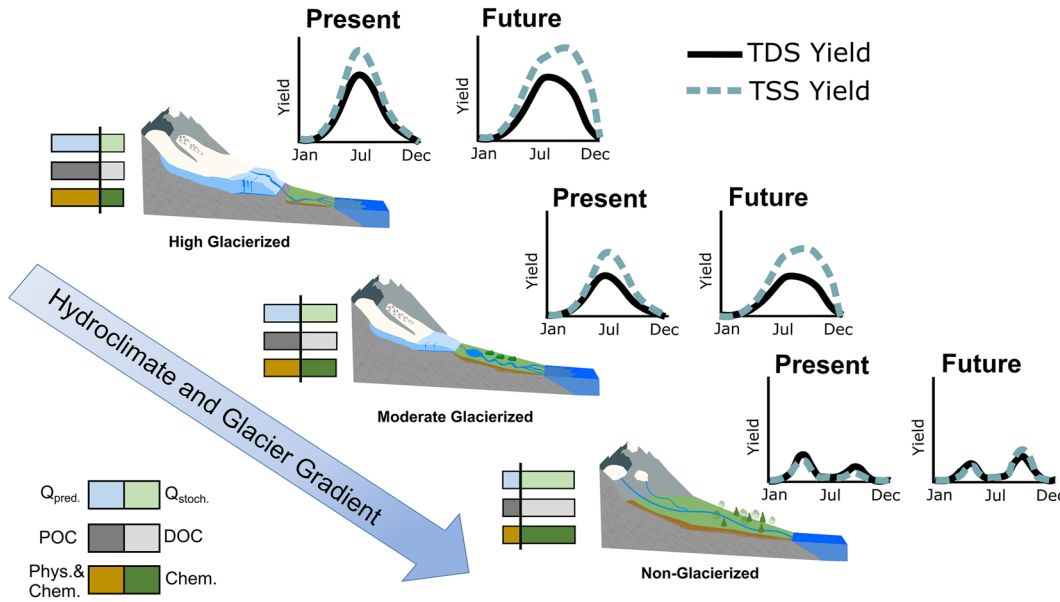

Figure 9. Conceptual model illustrating hypothesized changes to yields of TDS and TSS in the future using a gradient of glacier coverage and hydroclimate, such as KB and LC study regions as a guide. Hypothesized changes include the predictability of peak stream flow ($Q_{pred.}$ = predictable peak discharge, $Q_{stoch.}$ = stochastic discharge), POC:DOC and physical (Phys.) and chemical (Chem.) weathering regimes are illustrated by the position of the vertical black bar for each regime. Shifting from high to low glacierized catchment results in moving the bar to the left. Using the current conditions observed in the yields of Southeast Alaskan streams, we show how, across the GoA, yields of TSS and TDS may change seasonally from the present state observed in the KB region.

5.2. Seasonal Changes in Water Sources

An approach combining water stable isotope values and specific conductance (e.g., Figures 3 and 4) is extremely helpful in delineating seasonal changes in the sources of water contributing to stream flow. Within glacierized catchments, glacier melt contributes very low specific conductance water (Milner & Petts, 1994), and snow and glacier melt have depleted $\delta^{18}O$ values (Cable et al., 2011; Liu et al., 2004; Maurya et al., 2011; Penna et al., 2017; Schmieder et al., 2018). We found that the Grewingk and Mendenhall streams had distinct seasonal triangles compared to the other glacierized catchments. The presence of large proglacial lakes likely contributes to altering the variability due to the lake acting as a mixing zone and reservoir for the different waters. Within type 2 streams snowmelt dominates the transition between spring and summer evidenced by the decrease in specific conductance and depleted $\delta^{18}O$ values. Within the KB streams during the summer months, glacier melt continues to provide dilute water further decreasing the specific conductance and enriching the $\delta^{18}O$ values. However, the enrichment of $\delta^{18}O$ in LC streams is likely more influenced by precipitation given that the glacier ice endmember of LC glaciers is more depleted compared to the KB glacier ice endmember. We also observe that specific conductance in the LC type 2 streams continues to decrease into September while in KB streams specific conductance begins to increase after August. We hypothesize that the elevated precipitation in LC continues to provide a dilution effect into the fall. Type 3 streams comprise the non-glacierized watershed endmembers. The limited variability in $\delta^{18}O$ values indicate that the streams are primarily fed by a well-mixed source of snowmelt and rain. The elevated specific conductance values in the summer months indicate that a likely source of streamflow is provided by a slow flow or groundwater source.

The significance of groundwater as a source to streamflow within alpine catchments, both non-glacierized and glacierized, is gaining increased recognition (Liljedahl et al., 2017; Mackay et al., 2020; Somers & McKenzie, 2020). The alpine and post-glacial environment is replete with areas to store water including moraines, talus, alluvium, alluvial fans, and fractured bedrock (Somers & McKenzie, 2020). Water is stored and is eventually released, allowing for interaction with soils and bedrock before entering the stream through shallow and deep flow paths (Frisbee et al., 2017). These stored waters can support stream flow during times of low input and therefore may be an important part in the hydrologic and geochemical cycles (Engel et al., 2016; Penna et al., 2017). Sheep Creek (0% glacier) in the LC region had some of the highest yields of TDS compared to

the larger glacierized catchments within the region. During peak snowmelt, the TDS yields were at a seasonal maximum (Figure 7b). Similarly, during the fall when rain events are at a maximum, there is another increase in yields. We also observed that the concentrations of TDS and the specific conductance in Sheep Creek remained relatively stable throughout the season, which hints at the importance of continual groundwater contributions.

5.3. Regional Controls on Dissolved and Suspended Concentrations

Major elements and anions dominate the dissolved load in freshwater delivered via the terrestrial system to the intertidal ecosystem. In these watersheds the glacier coverage, lithology (mineralogy), and weathering rates/soil accumulation are the primary variables influencing the dissolved loads of stream waters. Specifically, it appears that the dissimilarity in concentrations of TDS between KB and LC can be attributed to lithology, soil thickness, soil maturity, and soil weathering profiles in the catchments. Lithologies in KB are primarily sedimentary with minor amounts of igneous rock whereas, the LC region has predominately igneous with lesser amounts of sedimentary rock. Therefore, as expected the extensive sedimentary bedrock in KB results in a higher weathering rates (Bluth & Kump, 1994) and higher solute concentrations. Based primarily on observations while in the field and the glacial history (Wiles & Calkin, 1990, 1994) the KB watersheds contain relatively thin, young soils, while the soils in LC are more mature and have undergone extensive weathering driven by the hydroclimate of the region (D'Amore et al., 2012; D'Amore, Ping, & Herendeen, 2015). Given that we sampled within a wide range of glacier coverages across the two study regions we attribute the higher concentrations of TDS in KB largely to the predominance of sedimentary lithology, and soils that have not weathered as intensely as in the LC region.

The elevated DOC concentrations in LC watersheds compared to KB is most easily accounted for due to the higher percentage of forest and wetlands in the LC region. In non-glacier fed Jakolof (KB) DOC concentrations are generally higher compared to the glacier fed streams. Conversely, non-glacierized Sheep Creek (LC) had lower DOC concentrations compared to the glacierized streams in LC (Figures 4 and 6), likely because of the low watershed wetland and forest coverage (Table 1). The highest observed DOC concentrations were from samples taken during the spring and fall in both regions attributable to flushing caused by snowmelt in the spring and precipitation in the fall (Fellman et al., 2020, 2009; Hood & Berner, 2009; Stewart et al., 2022).

Across the KB and LC region TSS concentrations are driven by glacier coverage (Figure 6 and Table 2) with expected higher concentrations occurring in the most glacierized watersheds. Previous work has shown that watersheds with >30% glacier coverage can have an order of magnitude more suspended sediment compared to a non-glacierized watershed (Hallet et al., 1996; Hood et al., 2020). The hydroclimate within LC, however, plays an important role in extending the high concentrations of TSS into late fall. During the melt season a distributed channelized system develops within glaciers which generally liberates more material (Fountain & Walder, 1998; Kohler et al., 2017; Swift et al., 2002). Therefore, in the late summer and fall as precipitation as rain increases in the LC region, rain water and glacier melt can entrain more material and increased soil erosion enhanced by large precipitation events can also contribute larger TSS loads.

5.4. Dissolved and Suspended Yields Driven by Hydroclimate and Glacier Coverage

The seasonal cycles in TDS yields at KB sites are similar to many other studies focused on the effects of glaciers on solute yields (Anderson et al., 2003; Hindshaw et al., 2011; Yde et al., 2014). Yields of TDS in KB peak during the height of the melt season, occur on average in July. Similar to recent work by Bergstrom et al. (2021) in an isolated and small glacierized watershed near Prince William Sound Alaska, the TDS yields in LC are elevated, and in many of the streams, peak in the late summer and fall. LC receives nearly double the amount of precipitation as KB, with much of it occurring during the late summer and fall and (Figure 1) sustaining higher streamflow during this time, a main driver of the solute yields. Because of the overall dominance of crystalline igneous rock and lack of carbonate minerals, chemical weathering is likely limited in the LC watersheds (Anderson et al., 1997; Urra et al., 2019). During periods of heavy rain, soil water and groundwater may be flushed from the watershed temporarily increasing solute loads (Stewart et al., 2022).

We observed three primary distinctions in DOC yields between the regions: (a) they are highest in the LC region; (b) peak yields in KB were observed primarily in July but there is a spring and a fall peak in LC; and (c) glacierized watersheds had the highest DOC yields. This last point is in contrast to previous work within Southeast Alaska watersheds that indicate DOC yields from non-glacierized watersheds are elevated compared to

glacierized watersheds (Hood et al., 2020; Hood & Scott, 2008), which has been attributed to glacier recession and the development of wetlands, soils, and forests. In our small subset of watersheds, we observed that the glacierized catchments had higher DOC yields. The glacierized watersheds also contain the highest wetland coverages which can be a large source of DOC, especially during high flow events induced by precipitation (D'Amore, Edwards, et al., 2015; Fellman et al., 2020). Therefore, the sites chosen for this study skew our results because the non-glacierized watersheds are small with topography that limits the development of characteristics (wetlands) that provide sources of DOC. To better characterize DOC dynamics within the GoA future studies should focus on selecting sites within many different types of watersheds that are across hydroclimate, glacial, elevation, and topography gradients.

As expected all glacierized watersheds had the highest yields of TSS. Glacier coverage is a primary driver of TSS yields (Hallet et al., 1996); however, regional climate may alter the seasonal cycles of those yields. We observed a continuous increase in TSS yields in the majority of LC streams from spring to fall. This pattern is dissimilar compared to KB streams, which had peak TSS yield in August with a subsequent decline into fall. The elevated streamflow and rain events in the fall in the LC region propel greater TSS yields comparatively later into the year.

5.5. Regional and Seasonal Controls on POC

The seasonality of $\delta^{13}C_{POC}$ of both regions provides several insights into regional stream dynamics. Enrichment in the $\delta^{13}C_{POC}$ values observed in many of the glacier fed streams (Figure 5) in both KB and LC indicate the POC values shift throughout the melt season from a depleted to an enriched source. The $\delta^{13}C_{POC}$ values for biogenic material should be relatively depleted compared to petrogenic sources (Hilton, 2017; Hood et al., 2020). Within Herbert, Lemon, and to some extent Cowee the $\delta^{13}C_{POC}$ values became enriched from spring through October, essentially matching the seasonal cycle of TSS (Figure 6). Non-glacierized Sheep Creek in LC had the most depleted $\delta^{13}C_{POC}$ values and limited changes from spring to fall, likely reflecting a continuous biogenic source of POC throughout the season. The enriched $\delta^{13}C_{POC}$ values in August and subsequent depletion in the KB streams indicate that the sediment sources continually shifted, likely due to a dominance of rock derived sources throughout the summer and an increase in biogenic sources in the fall. The difference between the two regions in the seasonal cycles of $\delta^{13}C_{POC}$ may indicate that in glacierized areas that receive heavy rain during the fall, sediment derived from glacial erosion is continually supplied which expands the temporal range of petrogenic POC delivery to the ocean which may have impacts on the coastal ecosystems.

5.6. Conceptualization of Future Changes in Solute and Sediment Yield to the GoA

Current projections of climate changes in the GoA region show an increase in precipitation, primarily in the form of rain in the fall and winter with lower annual snowfall and associated snowpack (Beamer et al., 2017; Littel et al., 2018). These projections in combination with receding glaciers will alter the seasonal flux of riverine freshwater and associated solutes and sediment to the GoA. As such, it is important to explore how current yields of solutes and sediment vary across the GoA. The Southeast region of Alaska receives some of the highest amounts of precipitation in Alaska and is a heavily glacierized region. Therefore, seasonal solute and sediment flux yields are shifted compared to the other regions in the GoA (Figure S6 in Supporting Information S1; see also Text S3 in Supporting Information S1). Within the majority of streams across the other regions TDS and TSS yields peak in July or August and quickly decline into the fall. Yields of TDS and TSS in Southeast streams follow a similar pattern into late summer, however, yields remain relatively elevated into mid fall, and in the case of TSS are elevated compared to the summer months (Figure S6c in Supporting Information S1). If we consider a situation where Southeast Alaska is a proxy for the future hydroclimate and seasonal freshwater yields, we can project a scenario of how future yields of solutes and sediments in the coming century across the GoA. Interestingly, though outside the period of study, both Southeast and Southcentral Alaska experienced their wettest years on record in 2022.

We hypothesize how future yields of solutes and sediments may change based on climate projections (Figure 9) in the coming century and offer three scenarios. Each scenario shows how discharge, POC:DOC ratios, physical and chemical weathering, TDS, and TSS may shift from the present state to a future state within basins of different amounts of glacier coverage and general watershed evolution as glaciers recede. The future state is based on the forecasted climate models which predict less snow, and more rain in the fall and winter. First, we address changes

in TDS and TSS. The first scenario illustrates how riverine transport in a heavily glacierized basin may change from the present. Snow melt and glacier melt will drive a peak in yields of TDS and TSS in the summer, however, increased fall rains will sustain yields later into the fall. Similarly, the second scenario with a moderately glacierized stream, yields will peak in July and August and be sustained into the fall; however, the yield will overall decrease due to lower glacier coverage. Finally, a previously glacierized basin with no current glacial ice will have two peaks in TDS and TSS yields, one driven by snow melt in the spring and another in the fall due to rain. As precipitation regimes change, the yields in the spring will decline caused by lower seasonal snowpack. However, TDS and TSS yields will likely increase in the fall attributed to increased fall rain. In this final scenario, rainfall and groundwater storage will become imminently important as water sources in these catchments.

We also illustrate how seasonal discharge, POC:DOC, and physical versus chemical weathering may change as a function of glacier recession. As glaciers recede the seasonal variability of freshwater discharge will become more dependent on seasonal weather patterns and less determined by glacier melt which provides an important predictable buffer and seasonal peak in freshwater. Within our 10 study sites this can be observed when comparing the hydrographs of non-glacierized Jakolof and Sheep to the glacierized watersheds. The overall POC:DOC will likely decrease with glacier recession and subsequent watershed evolution as vegetation, soil, and wetlands develop. Finally, we hypothesize that physical weathering will decline as glacier coverage within a watershed decreases, along with an increase in the chemical to physical weathering ratio. This will alter the chemical composition of the dissolved loads, likely causing an increase in the concentrations of major and trace elements. Within glacierized watersheds suspended sediment versus the dissolved yield is elevated compared to non-glacierized streams (Jenckes et al., 2022). The TDS and TSS from Sheep Creek exemplify this paradigm, with relatively low TSS yields and high TDS concentrations and yields. Glacier recession will likely alter this ratio moving to a state wherein the dissolved yield will be proportionally higher than the suspended sediment yields. Currently, there is a limited understanding of how this shift in the suspended and dissolved load will affect downstream and coastal marine ecosystems.

6. Conclusions

The detailed descriptions of seasonal variations in solute, carbon, and sediment cycles and yields illustrate the utility of a holistic approach to studying variably glacierized watersheds from a terrestrial export standpoint. We find that in general, glaciers control the overall yield of solutes and sediments, however, the hydroclimate can act as a control on the seasonal timing of those yields. We show that across the GoA, major element and anion (i.e., TDS) concentrations can vary widely primarily driven by watershed characteristics such as lithology, and soil development. The greater amount of sedimentary rocks within the KB region, compared to LC, contributes to the higher concentrations and yields of TDS. Similarly, DOC and POC seasonal cycles and yields are also driven by hydroclimate variability and different watershed characteristics, such as wetland area, impact the magnitude of DOC yields. Higher wetland coverages suggest a large source of DOC with increased DOC yields during periods of high-flow (Wei et al., 2021). Using $\delta^{13}C_{POC}$ values we were able to discern how the sourcing of sediment changes seasonally but also importantly that there are major differences in POC and DOC between the study regions. As precipitation as rain increases, primarily into fall, it is expected that there will be a subsequent shift in the timing of solute and sediment yields to the GoA. This work provides a baseline for future investigations into solute and suspended material exports to the GoA and indicates the importance of conceptualizing and quantifying the variability in watershed characteristics and hydroclimate across regions. Additionally, future projections of solute and sediment yields to the coastal zone will need to account for watershed evolution as glaciers recede.

Conflict of Interest

The authors declare no conflicts of interest relevant to this study.

Data Availability Statement

Data used in this manuscript are made available at http://hdl.handle.net/11122/13099.

Acknowledgments
Funding for this research is provided by NSF award OIA-1757347 to Lee Ann Munk and others. Jordan Jenckes received support from the Sloan Indigenous Graduate Partnership Fellowship. We would also like to thank McKinley Wallace, Aeon Russo, and Ena Burr whose diligence in the field and lab made this work possible. Additionally, we thank James Schloemer, who accompanied us in the field and whose stimulating conversation helped inform our hypotheses.

References

Alaska Climate Research Center. (2022). Climate change in Alaska. Retrieved from https://akclimate.org/climate-change-in-alaska/
Alley, R. B., Cuffey, K. M., & Zoet, L. K. (2019). Glacial erosion: Status and outlook. *Annals of Glaciology*, *60*(80), 1–13. https://doi.org/10.1017/aog.2019.38

Anderson, S. P. (2005). Glaciers show direct linkage between erosion rate and chemical weathering fluxes. *Geomorphology*, *67*(1–2), 147–157. https://doi.org/10.1016/j.geomorph.2004.07.010

Anderson, S. P., Drever, J. I., & Humphrey, N. F. (1997). Chemical weathering in glacial environments. *Geology*, *25*(5), 399–402. https://doi.org/10.1130/0091-7613(1997)025<0399:CWIGE>2.3.CO

Anderson, S. P., Longacre, S. A., & Kraal, E. R. (2003). Patterns of water chemistry and discharge in the glacier-fed Kennicott River, Alaska: Evidence for subglacial water storage cycles. *Chemical Geology*, *202*(3–4), 297–312. https://doi.org/10.1016/j.chemgeo.2003.01.001

Arimitsu, M. L., Piatt, J. F., & Mueter, F. (2016). Influence of glacier runoff on ecosystem structure in Gulf of Alaska fjords. *Marine Ecology Progress Series*, *560*, 19–40. https://doi.org/10.3354/meps11888

Beamer, J. P., Hill, D. F., Arendt, A., & Liston, G. E. (2016). High-resolution modeling of coastal freshwater discharge and glacier mass balance in the Gulf of Alaska watershed. *Water Resources Research*, *52*(5), 3888–3909. https://doi.org/10.1002/2015WR018457

Beamer, J. P., Hill, D. F., McGrath, D., Arendt, A., & Kienholz, C. (2017). Hydrologic impacts of changes in climate and glacier extent in the Gulf of Alaska watershed. *Water Resources Research*, *53*(9), 7502–7520. https://doi.org/10.1002/2016WR020033

Bergstrom, A., Koch, J. C., O'Neel, S., & Baker, E. (2021). Seasonality of solute flux and water source chemistry in a coastal glacierized watershed undergoing rapid change: Wolverine glacier watershed, Alaska. *Water Resources Research*, *57*(11), e2020WR028725. https://doi.org/10.1029/2020WR028725

Bhatia, M. P., Kujawinski, E. B., Das, S. B., Breier, C. F., Henderson, P. B., & Charette, M. A. (2013). Greenland meltwater as a significant and potentially bioavailable source of iron to the ocean. *Nature Geoscience*, *6*(4), 274–278. https://doi.org/10.1038/ngeo1746

Bieniek, P. A., Walsh, J. E., Thoman, R. L., & Bhatt, U. S. (2014). Using climate divisions to analyze variations and trends in Alaska temperature and precipitation. *Journal of Climate*, *27*(8), 2800–2818. https://doi.org/10.1175/JCLI-D-13-00342.1

Bluth, G. J. S., & Kump, L. R. (1994). Lithologic and climatologic controls of river chemistry. *Geochimica et Cosmochimica Acta*, *58*(10), 2341–2359. https://doi.org/10.1016/0016-7037(94)90015-9

Bradely, D. C., Kusky, T. M., Haeussler, P. J., Karl, S. M., & Donley, D. T. (1999). Geologic map of the Seldovia quadrangle, south-central Alaska. U.S. Geological Survey Open-File Report OFR 99-18G.

Buma, B., & Barrett, T. M. (2015). Spatial and topographic trends in forest expansion and biomass change, from regional to local scales. *Global Change Biology*, *21*(9), 3445–3454. https://doi.org/10.1111/gcb.12915

Cable, J., Ogle, K., & Williams, D. (2011). Contribution of glacier meltwater to streamflow in the Wind River Range, Wyoming, inferred via a Bayesian mixing model applied to isotopic measurements. *Hydrological Processes*, *25*(14), 2228–2236. https://doi.org/10.1002/hyp.7982

Chandler, R. F., Jr. (1943). The time required for Podzol profile formation as evidenced by the Mendenhall glacier deposits near Juneau, Alaska. *Soil Science Society of America Journal*, *7*(C), 454–459. https://doi.org/10.2136/sssaj1943.036159950007000C0077x

D'Amore, D. V., Edwards, R. T., Herendeen, P. A., Hood, E., & Fellman, J. B. (2015). Dissolved organic carbon fluxes from hydropedologic units in Alaskan coastal temperate rainforest watersheds. *Soil Science Society of America Journal*, *79*(2), 378–388. https://doi.org/10.2136/SSSAJ2014.09.0380

D'Amore, D. V., Fellman, J. B., Edwards, R. T., Hood, E., & Ping, C. L. (2012). Hydropedology of the North American coastal temperate rainforest. In *Hydropedology* (pp. 351–380). Elsevier. https://doi.org/10.1016/B978-0-12-386941-8.00011-3

D'Amore, D. V., Ping, C.-L., & Herendeen, P. A. (2015). Hydromorphic soil development in the coastal temperate rainforest of Alaska. *Soil Science Society of America Journal*, *79*(2), 698–709. https://doi.org/10.2136/SSSAJ2014.08.0322

Dansgaard, W. (1964). Stable isotopes in precipitation. *Tellus*, *16*(1), 436–468. https://doi.org/10.1111/j.2153-3490.1964.tb00181.x

Deb, D., Butcher, J., & Srinivasan, R. (2015). Projected hydrologic changes under mid-21st century climatic conditions in a sub-arctic watershed. *Water Resources Management*, *29*(5), 1467–1487. https://doi.org/10.1007/s11269-014-0887-5

Edwards, R. T., D'Amore, D. V., Biles, F. E., Fellman, J. B., Hood, E. W., Trubilowicz, J. W., & Floyd, W. C. (2021). Riverine dissolved organic carbon and freshwater export in the eastern Gulf of Alaska. *Journal of Geophysical Research: Biogeosciences*, *126*(1), e2020JG005725. https://doi.org/10.1029/2020JG005725

Engel, M., Penna, D., Bertoldi, G., Dell'Agnese, A., Soulsby, C., & Comiti, F. (2016). Identifying run-off contributions during melt-induced run-off events in a glacierized alpine catchment. *Hydrological Processes*, *30*(3), 343–364. https://doi.org/10.1002/hyp.10577

Evans, W., Mathis, J. T., & Cross, J. N. (2014). Calcium carbonate corrosivity in an Alaskan inland sea. *Biogeosciences*, *11*(2), 365–379. https://doi.org/10.5194/bg-11-365-2014

Fellman, J. B., Hood, E., Behnke, M. I., Welker, J. M., & Spencer, R. G. M. (2020). Stormflows drive stream carbon concentration, speciation, and dissolved organic matter composition in coastal temperate rainforest watersheds. *Journal of Geophysical Research: Biogeosciences*, *125*(9), e2020JG005804. https://doi.org/10.1029/2020JG005804

Fellman, J. B., Hood, E., D'Amore, D. V., Edwards, R. T., & White, D. (2009). Seasonal changes in the chemical quality and biodegradability of dissolved organic matter exported from soils to streams in coastal temperate rainforest. *Biogeochemistry*, *95*(2–3), 277–293. https://doi.org/10.1007/s10533-009-9336-6

Fellman, J. B., Hood, E., Dryer, W., & Pyare, S. (2015). Stream physical characteristics impact habitat quality for Pacific Salmon in two temperate coastal watersheds. *PLoS One*, *10*(7), e0132652. https://doi.org/10.1371/journal.pone.0132652

Fellman, J. B., Hood, E., Raymond, P. A., Stubbins, A., & Spencer, R. G. M. (2015b). Spatial variation in the origin of dissolved organic carbon in snow on the Juneau Icefield, Southeast Alaska. *Environmental Science and Technology*, *49*(19), 11492–11499. https://doi.org/10.1021/acs.est.5b02685

Fellman, J. B., Hood, E., Spencer, R. G. M., Stubbins, A., & Raymond, P. A. (2014). Watershed glacier coverage influences dissolved organic matter biogeochemistry in coastal watersheds of Southeast Alaska. *Ecosystems*, *17*(6), 1014–1025. https://doi.org/10.1007/s10021-014-9777-1

Fleming, S. W. (2005). Comparative analysis of glacial and nival streamflow regimes with implications for lotic habitat quantity and fish species richness. *River Research and Applications*, *21*(4), 363–379. https://doi.org/10.1002/rra.810

Fountain, A. G., & Walder, J. S. (1998). Water flow through temperate glaciers. *Reviews of Geophysics*, *36*(3), 299–328. https://doi.org/10.1029/97RG03579

Frisbee, M. D., Tolley, D. G., & Wilson, J. L. (2017). Field estimates of groundwater circulation depths in two mountainous watersheds in the Western U.S. and the effect of deep circulation on solute concentrations in streamflow. *Water Resources Research*, *53*(4), 2693–2715. https://doi.org/10.1002/2016WR019553

Gardner, A. S., Moholdt, G., Cogley, J. G., Wouters, B., Arendt, A. A., Wahr, J., et al. (2013). A reconciled estimate of glacier contributions to sea level rise: 2003 to 2009. *Science*, *340*(6134), 852–857. https://doi.org/10.1126/SCIENCE.1234532/SUPPL_FILE/GARDNER.SM.PDF

Giesbrecht, I. J. W., Tank, S. E., Frazer, G. W., Hood, E., Gonzalez Arriola, S. G., Butman, D. E., et al. (2022). Watershed classification predicts streamflow regime and organic carbon dynamics in the Northeast Pacific coastal temperate rainforest. *Global Biogeochemical Cycles*, *36*(2). https://doi.org/10.1029/2021GB007047

Hallet, B., Hunter, L., & Bogen, J. (1996). Rates of erosion and sediment evacuation by glaciers: A review of field data and their implications. *Global and Planetary Change*, *12*(1–4), 213–235. https://doi.org/10.1016/0921-8181(95)00021-6

Hawkings, J. R., Benning, L. G., Raiswell, R., Kaulich, B., Araki, T., Abyaneh, M., et al. (2018). Biolabile ferrous iron bearing nonparticles in glacier sediments. *Earth and Planetary Science Letters*, *493*, 92–101. https://doi.org/10.1016/j.epsl.2018.04.022

Hilton, R. G. (2017). Climate regulates the erosional carbon export from the terrestrial biosphere. *Geomorphology*, *277*, 118–132. https://doi.org/10.1016/j.geomorph.2016.03.028

Hindshaw, R. S., Tipper, E. T., Reynolds, B. C., Lemarchand, E., Wiederhold, J. G., Magnusson, J., et al. (2011). Hydrological control of stream water chemistry in a glacial catchment (Damma Glacier, Switzerland). *Chemical Geology*, *285*(1–4), 215–230. https://doi.org/10.1016/j.chemgeo.2011.04.012

Hood, E., & Berner, L. (2009). Effects of changing glacial coverage on the physical and biogeochemical properties of coastal streams in southeastern Alaska. *Journal of Geophysical Research*, *114*(3), 1–10. https://doi.org/10.1029/2009JG000971

Hood, E., Fellman, J. B., & Spencer, R. G. M. (2020). Glacier loss impacts riverine organic carbon transport to the ocean. *Geophysical Research Letters*, *47*(19), 1–9. https://doi.org/10.1029/2020GL089804

Hood, E., & Scott, D. (2008). Riverine organic matter and nutrients in southeast Alaska affected by glacial coverage. *Nature Geoscience*, *1*(9), 583–587. https://doi.org/10.1038/ngeo280

Hugonnet, R., McNabb, R., Berthier, E., Menounos, B., Nuth, C., Girod, L., et al. (2021). Accelerated global glacier mass loss in the early twenty-first century. *Nature*, *592*(7856), 726–731. https://doi.org/10.1038/s41586-021-03436-z

IPCC. (2018). In V. Masson-Delmotte, P. Zhai, H.-O. Pörtner, D. Roberts, J. Skea, P. R. Shukla, et al. (Eds.), *Global warming of 1.5°C. An IPCC Special Report on the impacts of global warming of 1.5°C above pre-industrial levels and related global greenhouse gas emission pathways, in the context of strengthening the global response to the threat of climate change, sustainable development, and efforts to eradicate poverty* (616 pp.). Cambridge University Press. https://doi.org/10.1017/9781009157940

Jenckes, J., Ibarra, D. E., & Munk, L. A. (2022). Concentration-discharge patterns across the Gulf of Alaska reveal geomorphological and glacierization controls on stream water solute generation and export. *Geophysical Research Letters*, *49*(1), e2021GL095152. https://doi.org/10.1029/2021GL095152

Johnson, M. A. (2021). Subtidal surface circulation in lower Cook Inlet and Kachemak Bay, Alaska. *Regional Studies in Marine Science*, *41*, 101609. https://doi.org/10.1016/J.RSMA.2021.101609

Kelly, B. P., Ainsworth, T., Boyce, D. A., Jr., Hood, E., Murphy, P., & Powell, J. (2007). Climate change: Predicated impacts on Juneau. In *Report to: Scientific Panel on Climate Change City and Borough of Juneau*.

Kohler, T. J., Žárský, J. D., Yde, J. C., Lamarche-Gagnon, G., Hawkings, J. R., Tedstone, A. J., et al. (2017). Carbon dating reveals a seasonal progression in the source of particulate organic carbon exported from the Greenland Ice Sheet. *Geophysical Research Letters*, *44*(12), 6209–6217. https://doi.org/10.1002/2017GL073219

Koppes, M. N., & Montgomery, D. R. (2009). The relative efficacy of fluvial and glacial erosion over modern to orogenic timescales. *Nature Geoscience*, *2*(9), 644–647. https://doi.org/10.1038/ngeo616

Kusky, T. M., & Bradley, D. C. (1999). Kinematic analysis of mélange fabrics: Examples and applications from the McHugh complex, Kenai Peninsula, Alaska. *Journal of Structural Geology*, *21*(12), 1773–1796. https://doi.org/10.1016/S0191-8141(99)00105-4

Larsen, C. F., Burgess, E., Arendt, A. A., O'Neel, S., Johnson, A. J., & Kienholz, C. (2015). Surface melt dominates Alaska glacier mass balance. *Geophysical Research Letters*, *42*(14), 5902–5908. https://doi.org/10.1002/2015GL064349

Li, D., Lu, X., Overeem, I., Walling, D. E., Syvitski, J., Kettner, A. J., et al. (2021). Excpetional increases in fluvial sediment fluxes in a warmer and wetter High Mountain Asia. *Science*, *374*(6567), 599–603. https://doi.org/10.1126/science.abi9649

Liljedahl, A. K., Gädeke, A., O'Neel, S., Gatesman, T. A., & Douglas, T. A. (2017). Glacierized headwater streams as aquifer recharge corridors, subarctic Alaska. *Geophysical Research Letters*, *44*(13), 6876–6885. https://doi.org/10.1002/2017GL073834

Littel, J. S., McAfee, S. A., & Hayward, G. D. (2018). Alaska snowpack response to climate change: Statewide snowfall equivalent and snowpack water scenarios. *Water*, *10*(5), 668. https://doi.org/10.3390/w10050668

Liu, F., Williams, M. W., & Caine, N. (2004). Source waters and flow paths in an alpine catchment, Colorado Front Range, United States. *Water Resources Research*, *40*(9). https://doi.org/10.1029/2004WR003076

Mackay, J. D., Barrand, N. E., Hannah, D. M., Krause, S., Jackson, C. R., Everest, J., et al. (2020). Proglacial groundwater storage dynamics under climate change and glacier retreat. *Hydrological Processes*, *34*(26), hyp.13961–5473. https://doi.org/10.1002/hyp.13961

Maurya, A. S., Shah, M., Deshpande, R. D., Bhardwaj, R. M., Prasad, A., & Gupta, S. K. (2011). Hydrograph separation and precipitation source identification using stable water isotopes and conductivity: River Ganga at Himalayan foothills. *Hydrological Processes*, *25*(10), 1521–1530. https://doi.org/10.1002/hyp.7912

McClelland, J. W., Townsend-Small, A., Holmes, R. M., Pan, F., Stieglitz, M., Khosh, M., & Peterson, B. J. (2014). River export of nutrients and organic matter from the North Slope of Alaska to the Beaufort Sea. *Water Resources Research*, *50*(2), 1823–1839. https://doi.org/10.1002/2013WR014722

Milner, A. M., Khamis, K., Battin, T. J., Brittain, J. E., Barrand, N. E., Füreder, L., et al. (2017). Glacier shrinkage driving global changes in downstream systems. *Proceedings of the National Academy of Sciences*, *114*(37), 9770–9778. https://doi.org/10.1073/pnas.1619807114

Milner, A. M., & Petts, G. E. (1994). Glacial rivers: Physical habitat and ecology. *Freshwater Biology*, *32*(2), 295–307. https://doi.org/10.1111/j.1365-2427.1994.tb01127.x

Moore, R. D., Fleming, S. W., Menounos, B., Wheate, R., Fountain, A., Stahl, K., et al. (2009). Glacier change in Western North America: Influences on hydrology, geomorphic hazards and water quality. *Hydrological Processes*, *23*(1), 42–61. https://doi.org/10.1002/hyp.7162

Nagorski, S. A., Vermilyea, A. W., & Lamborg, C. H. (2021). Mercury export from glacierized Alaskan watersheds as influenced by bedrock geology, watershed processes, and atmospheric deposition. *Geochimica et Cosmochimica Acta*, *304*, 32–49. https://doi.org/10.1016/J.GCA.2021.04.003

Neal, E. G., Hood, E., & Smikrud, K. (2010). Contribution of glacier runoff to freshwater discharge into the Gulf of Alaska. *Geophysical Research Letters*, *37*(6), 1–6. https://doi.org/10.1029/2010GL042385

O'Neel, S., Hood, E., Bidlack, A. L., Fleming, S. W., Arimitsu, M. L., Arendt, A., et al. (2015). Icefield-to-ocean linkages across the northern Pacific coastal temperate rainforest ecosystem. *BioScience*, *65*(5), 499–512. https://doi.org/10.1093/biosci/biv027

Penna, D., Engel, M., Bertoldi, G., & Comiti, F. (2017). Towards a tracer-based conceptualization of meltwater dynamics and streamflow response in a glacierized catchment. *Hydrology and Earth System Sciences*, *21*(1), 23–41. https://doi.org/10.5194/hess-21-23-2017

Pfeffer, W. T., Arendt, A. A., Bliss, A., Bolch, T., Cogley, J. G., Gardner, A. S., et al. (2014). The Randolph Glacier Inventory: A globally complete inventory of glaciers. *Journal of Glaciology*, *60*(221), 537–552. https://doi.org/10.3189/2014JoG13J176

Radić, V., Bliss, A., Beedlow, A. C., Hock, R., Miles, E., & Cogley, J. G. (2014). Regional and global projections of twenty-first century glacier mass changes in response to climate scenarios from global climate models. *Climate Dynamics*, *42*(1–2), 37–58. https://doi.org/10.1007/s00382-013-1719-7

Raiswell, R., Tranter, M., Benning, L. G., Siegert, M., De'ath, R., Huybrechts, P., & Payne, T. (2006). Contributions from glacially derived sediment to the global iron (oxyhydr)oxide cycle: Implications for iron delivery to the oceans. *Geochimica et Cosmochimica Act*, *70*(11), 2765–2780. https://doi.org/10.1016/j.gca.2005.12.027

Reisdorph, S. C., & Mathis, J. T. (2014). The dynamic controls on carbonate mineral saturation states and ocean acidification in a glacially dominated estuary. *Estuarine, Coastal and Shelf Science*, *144*(1), 8–18. https://doi.org/10.1016/j.ecss.2014.03.018

Schmieder, J., Garvelmann, J., Marke, T., & Strasser, U. (2018). Spatio-temporal tracer variability in the glacier melt end-member — How does it affect hydrograph separation results? *Hydrological Processes*, *32*(12), 1828–1843. https://doi.org/10.1002/hyp.11628

Schroth, A. W., Crusius, J., Chever, F., Bostick, B. C., & Rouxel, O. J. (2011). Glacial influence on the geochemistry of riverine iron fluxes to the Gulf of Alaska and effects of deglaciation. *Geophysical Research Letters*, *38*(16), L16605. https://doi.org/10.1029/2011GL048367

Sergeant, C. J., Falke, J. A., Bellmore, R. A., Bellmore, J. R., & Crumley, R. L. (2020). A classification of streamflow patterns across the coastal Gulf of Alaska. *Water Resources Research*, *56*(2), 1–17. https://doi.org/10.1029/2019WR026127

Shanley, C. S., Pyare, S., Goldstein, M. I., Alaback, P. B., Albert, D. M., Beier, C. M., et al. (2015). Climate change implications in the northern coastal temperate rainforest of North America. *Climatic Change*, *130*(2), 155–170. https://doi.org/10.1007/S10584-015-1355-9/TABLES/

Somers, L. D., & McKenzie, J. M. (2020). A review of groundwater in high mountain environments. *WIREs Water*, *7*(6). https://doi.org/10.1002/wat2.1475

Stewart, B., Shanley, J. B., Kirchner, J. W., Norris, D., Adler, T., Bristol, C., et al. (2022). Streams as mirrors: Reading subsurface water chemistry from stream chemistry. *Water Resources Research*, *58*(1), e2021WR029931. https://doi.org/10.1029/2021WR029931

Swift, D. A., Nienow, P. W., Spedding, N., & Hoey, T. B. (2002). Geomorphic implications of subglacial drainage configuration: Rates of basal sediment evacuation controlled by seasonal drainage system evolution. *Sedimentary Geology*, *149*(1–3), 5–19. https://doi.org/10.1016/S0037-0738(01)00241-X

Thornton, M. M., Shrestha, R., Wei, Y., Thornton, P. E., Kao, S., & Wilson, B. E. (2022). *Daymet: Daily surface weather data on a 1-km grid for North America, Version 4*. ORNL DAAC. https://doi.org/10.3334/ORNLDAAC/2129

Urra, A., Wadham, J., Hawkings, J. R., Telling, J., Hatton, J. E., Yde, J. C., et al. (2019). Weathering dynamics under contrasting Greenland Ice Sheet catchments. *Frontiers of Earth Science*, *7*. https://doi.org/10.3389/feart.2019.00299

Valentin, M. M., Hogue, T. S., & Hay, L. E. (2018). Hydrologic regime changes in a high-latitude glacierized watershed under future climate conditions. *Water (Switzerland)*, *10*(2), 128. https://doi.org/10.3390/w10020128

Wei, X., Hayes, D. J., Fernandez, I., Zhao, J., Fraver, S., Chan, C., & Diao, J. (2021). Identifying key environmental factors explaining temporal patterns of DOC export from watersheds in the conterminous United States. *Journal of Geophysical Research: Biogeosciences*, *126*(5), e2020JG005813. https://doi.org/10.1029/2020JG005813

Whitney, E. J., Beaudreau, A. H., & Howe, E. R. (2018). Using stable isotopes to assess the contribution of terrestrial and riverine organic matter to diets of nearshore marine consumers in a glacially influenced estuary. *Estuaries and Coasts*, *41*(1), 193–205. https://doi.org/10.1007/s12237-017-0260-z

Wiles, G. C., & Calkin, P. E. (1990). Neoglaciation in the southern Kenai Mountains, Alaska. *Annals of Glaciology*, *14*, 319–322. https://doi.org/10.1017/s0260305500008831

Wiles, G. C., & Calkin, P. E. (1994). Late Holocene, high-resolution glacial chronologies and climate, Kenai Mountains, Alaska. *Geological Society of America Bulletin*, *106*(2), 281–303. https://doi.org/10.1130/0016-7606(1994)106<0281:LHHRGC>2.3.CO;2

Wilson, F. H., Hults, C. P., Mull, C. G., & Karl, S. M. (2015). Geologic map of Alaska: U.S. Geological Survey Scientific Investigations Map 3340, pamphlet 196 p., 2 sheets, scale 1:1,584,000. https://doi.org/10.3133/sim3340

Yang, R., Hock, R., Kang, S., Shangguan, D., & Guo, W. (2020). Glacier mass and area changes on the Kenai Peninsula, Alaska, 1986–2016. *Journal of Glaciology*, *66*(258), 603–617. https://doi.org/10.1017/jog.2020.32

Yde, J. C., Knudsen, N. T., Hasholt, B., & Mikkelsen, A. B. (2014). Meltwater chemistry and solute export from a Greenland Ice Sheet catchment, Watson River, West Greenland. *Journal of Hydrology*, *519*(PB), 2165–2179. https://doi.org/10.1016/j.jhydrol.2014.10.018

Young, J. C., Pettit, E., Arendt, A., Hood, E., Liston, G. E., & Beamer, J. (2021). A changing hydrological regime: Trends in magnitude and timing of glacier ice melt and glacier runoff in a high latitude coastal watershed. *Water Resources Research*, *57*(7), e2020WR027404. https://doi.org/10.1029/2020WR027404

Zhang, T., Dongfeng, L., East, A. E., Walling, D. E., Lane, S., Overeem, I., et al. (2022). Warming-driven erosion and sediment transport in cold regions. *Nature Reviews Earth & Environment*, *3*(12), 832–851. https://doi.org/10.1038/s43017-022-00362-0